CANADA
DEPARTMENT OF ENERGY, MINES AND RESOURCES
Dominion Observatories

PUBLICATIONS

of the

DOMINION OBSERVATORY

OTTAWA

Volume XXXV • No. 8

ELECTROMAGNETIC INDUCTION ON A CONDUCTOR BOUNDED BY AN INCLINED SURFACE

T. Yukutake

Price 25 cents

ROGER DUHAMEL, F.R.S.C.
QUEEN'S PRINTER AND CONTROLLER OF STATIONERY
OTTAWA, 1967

Electromagnetic Induction in a Conductor Bounded by an Inclined Interface

T. Yukutake*

Abstract—Electromagnetic induction is studied for a two-dimensional earth model where a top conducting layer is underlain by a different tilted conductor. The problem is solved for a small angle of tilt by a successive approximation method, following repeated reflections of electromagnetic energy between the ground surface and the tilted boundary.

Two types of field are formulated within a conductor. One is characterized by having a vertical component of the magnetic field and the other by having no vertical component of the magnetic field. Both types of field are generated when either type of field arrives at the tilted boundary. It appears that the latter type field plays an important role in producing an anisotropic variation in the electromagnetic field.

Solutions are computed numerically on an electronic computer. Several examples of anisotropic behaviour of the electromagnetic field are shown.

Résumé—L'auteur étudie l'induction électromagnétique sur un modèle de Terre à deux dimensions, où une couche conductrice supérieure repose sur un conducteur incliné différent. Pour une faible inclinaison, le problème est résolu à l'aide d'une méthode par approximations successives, consécutive à un réfléchissement répété d'énergie électromagnétique entre la surface du sol et la limite inclinée.

Deux genres de champs sont induits dans un conducteur. L'un deux est caractérisé par une composante verticale du champ magnétique, tandis que l'autre n'en possède pas. Les deux genres de champs sont produits lorsque l'un d'eux atteint le plan incliné. Il semble que le dernier joue un rôle important dans la production d'une variation anisotropique du champ électromagnétique.

Les solutions sont calculées numériquement à l'aide d'un ordinateur électronique. L'auteur donne plusieurs exemples du comportement anisotropique du champ électromagnétique.

*Now at the Earthquake Research Institute, University of Tokyo, Tokyo, Japan.

1. Introduction

Theoretical work in magnetic induction and magnetotellurics has usually been based on horizontally stratified homogeneous structures (Cagniard 1953, Price 1962, Wait 1962). However, a number of observations by various investigators have revealed that the natural electromagnetic fluctuations are, at many places, much more complicated than may be expected from these theoretical results.

It has been frequently observed that the magnetic variation vectors have a tendency to confine themselves more or less on a plane which is a property of the observation point. (Parkinson 1959, 1962, 1964; Maeda et al., 1964; Horton 1965; Schmucker 1964; Lambert and Caner 1965). It is also reported at various stations that the vertical component of the magnetic field varies in phase with a particular component of the horizontal magnetic field irrespective of the orientation of the externally applied field. (Rikitake, 1959, 1964, 1966; Whitham and Andersen, 1962; Kertz, 1964; Schmucker, 1964; Simeon and Sposito, 1964). An anisotropic property of the telluric field variation has been observed at several places (Niblett and Sayn-Wittgenstein 1960; Srivastava et al., 1963). In extreme cases, the telluric field variations show a strong tendency to become linearly polarized while the magnetic variations are more or less unaffected (Yoshimatsu 1957; Yokoyama 1961, 1962; Rikitake and Sawada 1962; Whitham and Andersen 1965; Rikitake and Sawada 1962; Whitham and Andersen 1965; Rikitake 1966).

These unusual characteristics of the magnetic field and the anisotropic character of the telluric variation, especially the strong polarization of the telluric field, appear impossible to understand on the assumption of horizontally stratified homogeneous earth models.

Anomalous variations in the magnetic field generally are explained by inhomogeneities in the electrical conductivity within the earth and may be produced, for example, by electric currents concentrated in highly conductive regions embodied in a poorly conductive earth (Rikitake 1966; Whitham and Andersen 1962; Law et al., 1963; Kertz 1964; Schmucker 1964) or the edge effect between the ocean and the land (Parkinson, 1962, 1964; Weaver 1963; Schmucker 1964). On the other hand, anisotropic variations of the telluric field usually are discussed in terms of possible anisotropy of electrical conductivity (Rikitake and Sawada 1962; Yokoyama 1961, 1962; Whitham and Andersen 1965), whereas only a few studies have been made of the inhomogeneous distribution of different conductors.

D'Erceville and Kunetz (1962) discussed the effect of a fault on the natural electromagnetic field in the case where the fault is the boundary between two different conductors. Although their study was limited to a particular type of field specified by the electric vector having only a component normal to the fault, they concluded that the electric field on the more conductive slide diminishes rapidly on approaching the fault. Mann (1964) studied the magnetotelluric problem, using the perturbation method, when the conductor was bounded by a sinusoidal surface under the ground, and obtained an anisotropic property of the electromagnetic field. Unfortunately, however, these theories are not sufficiently comprehensive to be applicable to anisotropic phenomena characterized by periods of a few minutes to several hours because particular types of plane waves were assumed as the external field, whereas the variations actually observed at such moderate periods are composed of a more complicated field than that expressed by simple plane waves.

In this paper, electromagnetic induction at the surface of an inclined conductor is discussed when the external field has a wave length of finite extent. Discussion is limited to problems where the angle of tilt of the boundary is small and the effect of the intersection point of the ground surface with the inclined discontinuity is ignored.

In section 2, two types of electromagnetic field in the conductor are formulated. In section 3, the induction problem for horizontal structures is briefly discussed when the two different types of electromagnetic field are taken into considerration. The same procedures discussed in section 3 are extended to the problem of tilted boundary in section 4. Results of numerical calculations for tilted boundary problems are shown in section 5.

2. Two Types of Electromagnetic Field within a Conductor.

When the time factor is assumed to be $e^{i\omega t}$, Maxwell's equations can be written in electromagnetic units as follows,

$$\left.\begin{aligned} \text{curl } \mathbf{H} &= \frac{k^2}{i\omega\mu}\mathbf{E} \\ \text{curl } \mathbf{E} &= -i\omega\mu\mathbf{H} \\ \text{div } \mathbf{H} &= 0 \\ \text{div } \mathbf{E} &= 4\pi\rho\frac{c^2}{\epsilon} \end{aligned}\right\} \quad (2.1)$$

where $\mathbf{H}$ is the magnetic field vector, $\mathbf{E}$ the electric field, μ the magnetic permeability, ϵ the dielectric constant, ρ the charge density, c the velocity of light, σ the electrical conductivity and

$$k^2 = 4\pi\sigma\mu\omega i + \frac{\epsilon\mu}{c^2}\omega^2 \quad (2.2)$$

It may be assumed that the density of free charge in the conductor is always zero, because the relaxation time of charge is extremely short in the interior. Then we have

$$\text{div } \mathbf{E} = 0 \quad (2.3)$$

Under this condition, Maxwell's equations can be reduced to the following form,

$$\nabla^2\mathbf{H} - k^2\mathbf{H} = 0 \quad (2.4)$$

$$\nabla^2\mathbf{E} - k^2\mathbf{E} = 0 \quad (2.5)$$

The equation (2.4) has two different types of solutions (Price 1950; Bullard 1949), namely,

$$\mathbf{H}_T = \begin{bmatrix} \frac{\partial\psi}{\partial y} \\ -\frac{\partial\psi}{\partial x} \\ 0 \end{bmatrix} \quad (2.6)$$

and

$$\mathbf{H}_S = \frac{1}{ik}\begin{bmatrix} \frac{\partial^2\psi}{\partial x\partial z} \\ \frac{\partial^2\psi}{\partial y\partial z} \\ -\frac{\partial^2\psi}{\partial x^2} - \frac{\partial^2\psi}{\partial y^2} \end{bmatrix} \quad (2.7)$$

where ψ is the function which should satisfy the following equation.

$$\nabla^2\psi - k^2\psi = 0$$

Similarly, we have the following types of solutions for the electric field, corresponding to the magnetic field $\mathbf{H}_T$ and $\mathbf{H}_S$ respectively,

$$\mathbf{E}_S = \frac{i\omega\mu}{k^2}\begin{bmatrix} \frac{\partial^2\psi}{\partial x\partial z} \\ \frac{\partial^2\psi}{\partial y\partial z} \\ -\frac{\partial^2\psi}{\partial x^2} - \frac{\partial^2\psi}{\partial y^2} \end{bmatrix} \tag{2.8}$$

$$\mathbf{E}_T = -\frac{\omega\mu}{k}\begin{bmatrix} \frac{\partial\psi}{\partial y} \\ -\frac{\partial\psi}{\partial x} \\ 0 \end{bmatrix} \tag{2.9}$$

Henceforth we shall call ($\mathbf{H}_S$, $\mathbf{E}_T$) the first type field and ($\mathbf{H}_T$, $\mathbf{E}_S$) the second type field.

3. Electromagnetic Induction for Two Horizontally Stratified Layers.

3–1. Formulation of the electromagnetic field at the ground surface.

The induction problem of the second type field was discussed by Price (1950) with respect to a semi-infinite plane conductor. In his study he ignored the displacement current in the atmosphere. It followed that the magnetic field of the second type always became zero outside the earth. Then he concluded that the second type field inside the conductor corresponds to the free decay of certain distributions of electric current, which cannot be affected by any external (first type) field.

In this section, retaining the displacement current in a parameter k_1, we shall briefly discuss electromagnetic induction for an earth model of horizontal structure, including the second type field.

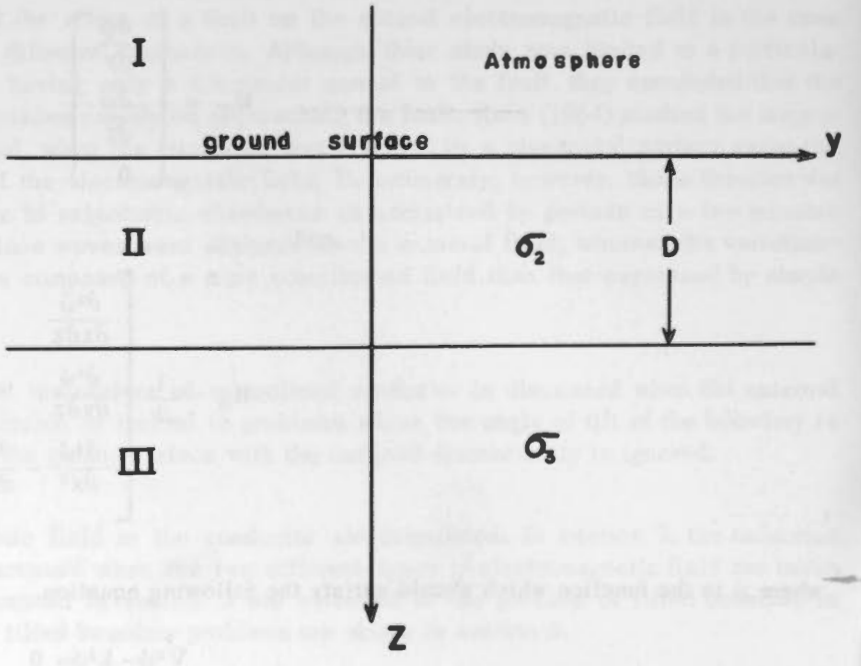

FIGURE 1. Model of horizontal structure.

Let us take the earth model as is shown in Figure 1. Then the first type field can be expressed from (2.7) and (2.9) as follows,

$$\mathbf{H}_S^{je} = \frac{1}{ik_j}\begin{bmatrix} -ip\sqrt{\nu^2+k_j^2} \\ -iq\sqrt{\nu^2+k_j^2} \\ \nu^2 \end{bmatrix} e^{ipx+iqy}\ e^{-\sqrt{\nu^2+k_j^2}\,z} \tag{3.1}$$

$$\mathbf{E}_T^{je} = -\frac{\omega\mu}{k_j}\begin{bmatrix} iq \\ -ip \\ 0 \end{bmatrix} e^{ipx+iqy}\ e^{-\sqrt{\nu^2+k_j^2}\,z} \tag{3.2}$$

$$\mathbf{H}_S^{ji} = \frac{1}{ik_j}\begin{bmatrix} ip\sqrt{\nu^2+k_j^2} \\ iq\sqrt{\nu^2+k_j^2} \\ \nu^2 \end{bmatrix} e^{ipx+iqy}\ e^{\sqrt{\nu^2+k_j^2}\,z} \tag{3.3}$$

$$\mathbf{E}_T^{ji} = -\frac{\omega\mu}{k_j}\begin{bmatrix} iq \\ -ip \\ 0 \end{bmatrix} e^{ipx+iqy}\ e^{\sqrt{\nu^2+k_j^2}\,z} \tag{3.4}$$

$$k_j^2 = 4\pi\sigma_j\mu_j\omega i + \frac{\epsilon_j\mu_j}{c^2}\omega^2 \tag{3.5}$$

$$\nu^2 = p^2 + q^2 \tag{3.6}$$

Where suffix j indicates the quantity in the j–th layer. $\mathbf{H}_S^{je}$ represents the first type magnetic field of external origin in the j–th layer, $\mathbf{H}_S^{ji}$ the first type magnetic field of internal origin. Similarly $\mathbf{E}_T^{je}$ and $\mathbf{E}_T^{ji}$ are the first type electric field of external and internal origin respectively. The explicit forms of the second type field are derivable from (2.6) and (2.8) as follows,

$$\mathbf{H}_T^{je} = \begin{bmatrix} iq \\ -ip \\ 0 \end{bmatrix} e^{ipx+ipy}\ e^{-\sqrt{\nu^2+k_j^2}\,z} \tag{3.7}$$

$$\mathbf{E}_S^{je} = \frac{i\omega\mu}{k_j^2}\begin{bmatrix} -ip\sqrt{\nu^2+k_j^2} \\ -iq\sqrt{\nu^2+k_j^2} \\ \nu^2 \end{bmatrix} e^{ipx+iqy}\ e^{-\sqrt{\nu^2+k_j^2}\,z} \tag{3.8}$$

$$\mathbf{H}_T^{ji} = \begin{bmatrix} iq \\ -ip \\ 0 \end{bmatrix} e^{ipx+iqy}\ e^{\sqrt{\nu^2+k_j^2}\,z} \tag{3.9}$$

$$\mathbf{E}_S^{ji} = \frac{i\omega\mu}{k_j^2}\begin{bmatrix} ip\sqrt{\nu^2+k_j^2} \\ iq\sqrt{\nu^2+k_j^2} \\ \nu^2 \end{bmatrix} e^{ipx+iqy}\ e^{\sqrt{\nu^2+k_j^2}\,z} \tag{3.10}$$

The electromagnetic field within each layer is composed of the above different types of the field. In the region (I), the magnetic field and the electric field can be expressed in the following forms.

$$\left.\begin{aligned} \mathbf{H} &= A_{1S}\mathbf{H}_S^{1e} + B_{1S}\mathbf{H}_S^{1i} + A_{1T}\mathbf{H}_T^{1e} + B_{1T}\mathbf{H}_T^{1i} \\ \mathbf{E} &= A_{1S}\mathbf{E}_T^{1e} + B_{1S}\mathbf{E}_T^{1i} + A_{1T}\mathbf{E}_S^{1e} + B_{1T}\mathbf{E}_S^{1i} \end{aligned}\right\} \quad \text{for (I)} \tag{3.11}$$

where A_{1S}, A_{1T}, B_{1S} and B_{1T} are constants to be determined from boundary conditions. Similarly we have,

$$\left.\begin{aligned} \mathbf{H} &= A_{2S}\mathbf{H}_S^{2e} + B_{2S}\mathbf{H}_S^{2i} + A_{2T}\mathbf{H}_T^{2e} + B_{2T}\mathbf{H}_T^{2i} \\ \mathbf{E} &= A_{2S}\mathbf{E}_T^{2e} + B_{2S}\mathbf{E}_T^{2i} + A_{2T}\mathbf{E}_S^{2e} + B_{2T}\mathbf{E}_S^{2i} \end{aligned}\right\} \quad \text{for (II)} \qquad (3.12)$$

and

$$\left.\begin{aligned} \mathbf{H} &= A_{3S}\mathbf{H}_S^{3e} + A_{3T}\mathbf{H}_T^{3e} \\ \mathbf{E} &= A_{3S}\mathbf{E}_T^{3e} + A_{3T}\mathbf{E}_S^{3e} \end{aligned}\right\} \quad \text{for (III)} \qquad (3.13)$$

Since the electrical conductivity of each layer is finite, tangential components of the magnetic field, the normal component of the magnetic flux density and the tangential components of the electric field are required to be continuous at each boundary. At the surface of the ground, for example, the following equations should be satisfied.

$$\left.\begin{aligned}
&\frac{1}{ik_1}\{A_{1S}(-ip\sqrt{\nu^2+k_1^2}) + B_{1S}(ip\sqrt{\nu^2+k_1^2})\} + \{A_{1T}(iq) + B_{1T}(iq)\} \\
&\quad = \frac{1}{ik_2}\{A_{2S}(-ip\sqrt{\nu^2+k_2^2}) + B_{2S}(ip\sqrt{\nu^2+k_2^2})\} + \{A_{2T}(iq) + B_{2T}(iq)\} \\
&\frac{1}{ik_1}\{A_{1S}(-iq\sqrt{\nu^2+k_1^2}) + B_{1S}(iq\sqrt{\nu^2+k_1^2})\} + \{A_{1T}(-ip) + B_{1T}(-ip)\} \\
&\quad = \frac{1}{ik_1}\{A_{2S}(-iq\sqrt{\nu^2+k_2^2}) + B_{2S}(iq\sqrt{\nu^2+k_2^2})\} + \{A_{2T}(-ip) + B_{2T}(-ip)\} \\
&\frac{1}{ik_1}\{A_{1S}\nu^2 + B_{1S}\nu^2\} = \frac{1}{ik_1}\{A_{2S}\nu^2 + B_{2S}\nu^2\} \\
&-\frac{\omega\mu}{k_1}\left[\{A_{1S}(iq) + B_{1S}(iq)\} + \frac{A_{1T}}{ik_1}(-ip\sqrt{\nu^2+k_1^2}) + \frac{B_{1T}}{ik_1}(ip\sqrt{\nu^2+k_1^2})\right] \\
&\quad = -\frac{\omega\mu}{k_2}\left[\{A_{2S}(iq) + B_{2S}(iq)\} + \frac{A_{2T}}{ik_2}(-ip\sqrt{\nu^2+k_2^2}) + \frac{B_{2T}}{ik_2}(ip\sqrt{\nu^2+k_2^2})\right] \\
&-\frac{\omega\mu}{k_1}\left[\{A_{1S}(-ip) + B_{1S}(-ip) + \frac{A_{1T}}{ik_1}(-iq\sqrt{\nu^2+k_1^2}) + \frac{B_{1T}}{ik_1}(iq\sqrt{\nu^2+k_1^2})\right] \\
&\quad = -\frac{\omega\mu}{k_2}\left[\{A_{2S}(-ip) + B_{2S}(-ip)\} + \frac{A_{2T}}{ik_2}(-iq\sqrt{\nu^2+k_2^2}) + \frac{B_{2T}}{ik_2}(iq\sqrt{\nu^2+k_2^2})\right]
\end{aligned}\right\} \qquad (3.14)$$

Then the first equation, for example, can be rewritten as follows,

$$-ip\left[\frac{1}{ik_1}\sqrt{\nu^2+k_1^2}(A_{1S}-B_{1S}) - \frac{1}{ik_2}\sqrt{\nu^2+k_2^2}(A_{2S}-B_{2S})\right]$$
$$+ iq\left[(A_{1T} + B_{1T}) - (A_{2T}+B_{2T})\right] = 0 \qquad (3.15)$$

p and q are independent of each other, since these quantities are dependent on the configuration of the external source field only. Consequently, in place of the above equation, we have the following two equations, each of which involves either the first or the second type field respectively.

$$\left.\begin{aligned} &\frac{1}{k_1}\sqrt{\nu^2+k_1^2}\,(A_{1S}-B_{1S}) - \frac{1}{k_2}\sqrt{\nu^2+k_2^2}\,(A_{2S}-B_{2S}) = 0 \\ &(A_{1T}+B_{1T}) - (A_{2T}+B_{2T}) = 0 \end{aligned}\right\} \quad (3.16)$$

In the same way, it can easily be proved that the first and the second type field should satisfy all the boundary conditions separately.

Solving the boundary conditions, we have the following results for the first type field.

$$\left.\begin{aligned} B_{1S} &= \frac{\sqrt{\nu^2+k_1^2}\,(1+\beta) - \sqrt{\nu^2+k_2^2}\,(1-\beta)}{\sqrt{\nu^2+k_1^2}\,(1+\beta) + \sqrt{\nu^2+k_2^2}\,(1-\beta)}\,A_{1S} \\ A_{2S} &= \frac{k_2}{k_1}\,\frac{2\sqrt{\nu^2+k_1^2}}{\sqrt{\nu^2+k_1^2}\,(1+\beta) + \sqrt{\nu^2+k_2^2}\,(1-\beta)}\,A_{1S} \\ B_{2S} &= \beta\, A_{2S} \\ A_{3S} &= \frac{k_3}{k_2}\,\frac{2\sqrt{\nu^2+k_2^2}\,e^{-\sqrt{\nu^2+k_2^2}\,D}}{(\sqrt{\nu^2+k_2^2} + \sqrt{\nu^2+k_3^2})\,e^{-\sqrt{\nu^2+k_3^2}\,D}}\,A_{2S} \\ \beta &= \frac{\sqrt{\nu^2+k_2^2} - \sqrt{\nu^2+k_3^2}}{\sqrt{\nu^2+k_2^2} + \sqrt{\nu^2+k_3^2}}\,e^{-2\sqrt{\nu^2+k_2^2}\,D} \end{aligned}\right\} \quad (3.17)$$

For the second type field, we have

$$\left.\begin{aligned} B_{1T} &= \frac{\frac{1}{k_1^2}\sqrt{\nu^2+k_1^2}\,(1+\alpha) - \frac{1}{k_2^2}\sqrt{\nu^2+k_2^2}\,(1-\alpha)}{\frac{1}{k_1^2}\sqrt{\nu^2+k_1^2}\,(1+\alpha) + \frac{1}{k_2^2}\sqrt{\nu^2+k_2^2}\,(1-\alpha)}\,A_{1T} \\ A_{2T} &= \frac{\frac{2}{k_1^2}\sqrt{\nu^2+k_1^2}}{\frac{1}{k_1^2}\sqrt{\nu^2+k_1^2}\,(1+\alpha) + \frac{1}{k_2^2}\sqrt{\nu^2+k_2^2}\,(1-\alpha)}\,A_{1T} \\ B_{2T} &= \alpha A_{2T} \\ A_{3T} &= \frac{\frac{2}{k_2^2}\sqrt{\nu^2+k_2^2}\,e^{-\sqrt{\nu^2+k_2^2}\,D}}{(\frac{1}{k_2^2}\sqrt{\nu^2+k_2^2} + \frac{1}{k_3^2}\sqrt{\nu^2+k_3^2})\,e^{-\sqrt{\nu^2+k_3^2}\,D}}\,A_{2T} \\ \alpha &= \frac{\frac{1}{k_3^2}\sqrt{\nu^2+k_2^2} - \frac{1}{k_3^2}\sqrt{\nu^2+k_3^2}}{\frac{1}{k_2^2}\sqrt{\nu^2+k_2^2} + \frac{1}{k_3^2}\sqrt{\nu^2+k_3^2}}\,e^{-2\sqrt{\nu^2+k_2^2}\,D} \end{aligned}\right\} \quad (3.18)$$

3–2. Magnetotelluric relationship for the two-layer model.

a) The first type field as an external field

When the first type field is applied from outside the earth, the ratio between orthogonal horizontal components of the electric and the magnetic field at the ground surface can be written as follows,

$$\frac{(E_{2T})_X}{(H_{2S})_Y} = \frac{i\omega\mu}{\sqrt{\nu^2+k_2^2}}\frac{1+\beta}{1-\beta}$$

$$= \frac{i\omega\mu}{\sqrt{\nu^2+k_2^2}}\frac{\sqrt{\nu^2+k_2^2}\,(1+e^{-2\sqrt{\nu^2+k_2^2}D})+\sqrt{\nu^2+k_3^2}\,(1-e^{-2\sqrt{\nu^2+k_2^2}D})}{\sqrt{\nu^2+k_2^2}\,(1-e^{-2\sqrt{\nu^2+k_2^2}D})+\sqrt{\nu^2+k_3^2}\,(1+e^{-2\sqrt{\nu^2+k_2^2}D})} \tag{3.19}$$

Similarly, the ratio of the vertical component of the horizontal component of the magnetic field is obtained as,

$$\frac{(H_{2S})_Z}{\{(H_{2S})_X, (H_{2S})_Y\}} = \frac{i\nu^2}{\{p,q\}\sqrt{\nu^2+k_2^2}}\frac{1+\beta}{1-\beta}$$

$$= \frac{i\nu^2}{\{p,q\}\sqrt{\nu^2+k_2^2}}\frac{\sqrt{\nu^2+k_2^2}\,(1+e^{-2\sqrt{\nu^2+k_2^2}D})+\sqrt{\nu^2+k_3^2}\,(1-e^{-2\sqrt{\nu^2+k_2^2}D})}{\sqrt{\nu^2+k_2^2}\,(1-e^{-2\sqrt{\nu^2+k_2^2}D})+\sqrt{\nu^2+k_3^2}\,(1+e^{-2\sqrt{\nu^2+k_2^2}D})} \tag{3.20}$$

In the case when k_3 is extremely large ($k_3^2 \gg \nu^2$, $k_3^2 \gg k_2^2$) and $\sqrt{\nu^2+k_2^2}\,D \ll 1$, the above equation (3.19) can be simplified as follows.

$$\frac{(E_{2T})_X}{(H_{2S})_Y} = i\omega\mu D \tag{3.21}$$

The ratio of the electric to the magnetic field becomes independent of the conductivity of the II and III layer, and is simply proportional to the frequency ω and the depth to the conductor D. This is exactly the same result obtained by Cagniard (1953).

Under the same conditions, the ratio of the vertical to the horizontal component of the magnetic field can be reduced to

$$\frac{(H_{2S})_Z}{\{(H_{2S})_X, (H_{2S})_Y\}} = \frac{i\nu^2}{\{p,q\}}D \tag{3.22}$$

This quantity is subject to a configuration of the source field in terms of ν^2/p or ν^2/q. However, in the case when the wave length of the external field has been estimated by independent means, a straightforward estimate of the depth D becomes possible by (3.22).

In the case where a poor conductor is overlain by a moderate conducting layer, namely $k_3 \ll 1$, and k_2D is also small when $\nu \ll 1$, (3.19) becomes

$$\frac{(E_{2T})_X}{(H_{2S})_Y} = \frac{1}{4\pi\sigma_2 D} \tag{3.23}$$

The ratio of the electric to the magnetic field becomes independent of frequency in this case, and is inversely proportional to the top layer conductivity σ_2 and the depth D, as has already been pointed out by Cagniard (1953) and Price (1962).

Under the same conditions, we have from (3.20)

$$\frac{(H_{2S})_Z}{\{(H_{2S})_X, (H_{2S})_Y\}} = \frac{\nu^2}{\{p, q\}} \cdot \frac{1}{4\pi\sigma_2\omega D} \tag{3.24}$$

which is dependent on the frequency as well as the source field configuration.

These relations may be useful for a rough estimation of the conductivity (σ_2) of the top layer when it is overlying a poor conductor.

b) The second type field as an external field

Corresponding to (3.19), the ratio of the electric to the magnetic field at the ground surface can be represented as follows,

$$\frac{(E_{2S})_X}{(H_{2T})_Y} = i\omega\mu \frac{\sqrt{\nu^2+k_2^2}}{k_2^2} \frac{1-\alpha}{1+\alpha}$$

$$= i\omega\mu \frac{\sqrt{\nu^2+k_2^2}}{k_2^2} \frac{\frac{1}{k_2^2\sqrt{\nu^2+k_2^2}}(1-e^{-2\sqrt{\nu^2+k_2^2}D}) + \frac{1}{k_3^2\sqrt{\nu^2+k_3^2}}(1+e^{-2\sqrt{\nu^2+k_2^2}D})}{\frac{1}{k_2^2\sqrt{\nu^2+k_2^2}}(1+e^{-2\sqrt{\nu^2+k_2^2}D}) + \frac{1}{k_3^2\sqrt{\nu^2+k_3^2}}(1-e^{-2\sqrt{\nu^2+k_3^2}D})} \tag{3.25}$$

In the case where σ_3 is large ($k_3^2 \gg \nu^2$, $k_3^2 \gg k_2^2$, $k_2^2 \gg \nu^2$) and $\sqrt{\nu^2+k_2^2}\,D \ll 1$, we have

$$\frac{(E_{2S})_X}{(H_{2T})_Y} = i\omega\mu D \tag{3.26}$$

On the other hand, when σ_3 is small ($k_3^2 \ll 1$, $\nu^2 \ll k_2^2$) and the conductivity σ^2 is moderate so that the relationship $k_2 D \ll 1$ holds, then (3.25) becomes

$$\frac{(E_{2S})_X}{(H_{2T})_Y} = \frac{1}{4\pi\sigma_2 D} \tag{3.27}$$

These are identical with the results (3.21), (3.23) obtained for the first type.

3–3. Order of magnitude estimate of the two types of the field

A rough estimate of the magnitude of both types of field is made in this section, for the purpose of examining whether or not the second type field actually plays an important role when both types of the field are applied to the earth simultaneously.

The amplitude ratio of the second to the first type magnetic field becomes

$$\left.\begin{aligned} \frac{|H_T|_Y}{|H_S|_Y} &= \left[\frac{A_{2T}H_T^{2e} + B_{2T}H_T^{2i}}{A_{2S}H_S^{2e} + B_{2S}H_S^{2i}}\right]_{z=0} \\ &= \frac{p}{q}\frac{ik_1}{\sqrt{\nu^2+k_2^2}}\frac{1+\alpha}{1-\beta}\left\{\frac{1+\beta}{1+\alpha} + \frac{\sqrt{\nu^2+k_2^2}\,(1-\beta)}{\sqrt{\nu^2+k_1^2}\,(1+\alpha)}\right\}\frac{A_{1T}}{A_{1S}} \end{aligned}\right\} \tag{3.28}$$

$$= \begin{cases} 2i\dfrac{p}{q}\dfrac{k_1}{\nu}\dfrac{1}{1-\beta}\dfrac{A_{1T}}{A_{1S}} & \text{for } k_2^2 \ll \nu^2,\ k_1^2 \ll \nu^2 \\ i\dfrac{p}{q}\dfrac{k_1}{\nu}\dfrac{A_{1T}}{A_{1S}} & \text{for } k_2^2 \gg \nu^2 \gg k_1^2 \end{cases} \tag{3.29}$$

It is impossible to know, a priori, the intensity and the distribution of the external field. Therefore the ratio of A_{1T}/A_{1S} remains undetermined in the above equation. However, if we assume that A_{1T} and A_{1S} are the same order of magnitude, then the ratio of the second to the first type field becomes order of magnitude, k_1/ν. ν is usually larger than 10^{-9}cm^{-1} (Price 1962), and we may expect that k_1 should be less than 10^{-11}cm^{-1} for variations with periods longer than 1 min. Therefore k_1/ν is less than 10^{-2}. This indicates that the second type field is negligibly small compared with the first type field when the source field energy is equally distributed in both types of the field.

Similarly, the ratio of the second to the first type electric field at $z = 0$ becomes

$$\frac{|E_S|_Y}{|E_T|_Y} = \left[\frac{A_{2T}E_S^{2e} + B_{2T}E_S^{2i}}{A_{2S}E_T^{2e} + B_{2S}E_T^{2i}}\right]_{z=0}$$

$$= \frac{q}{p}\frac{\sqrt{\nu^2+k_2^2}\,(1-\alpha)}{ik_2}\frac{k_1}{(1+\beta)\,k_2}\left\{\frac{1+\beta}{1+\alpha} + \frac{\sqrt{\nu^2+k_2^2}}{\sqrt{\nu^2+k_1^2}}\frac{(1-\beta)}{(1+\alpha)}\right\}\frac{A_{1T}}{A_{1S}} \qquad (3.30)$$

$$= \begin{cases} -2i\,\dfrac{q}{p}\dfrac{k_1\nu}{k_2^2}\dfrac{1-\alpha}{(1+\alpha)(1+\beta)}\dfrac{A_{1T}}{A_{1S}} & \text{for } k_2^2 \ll \nu^2,\ k_1^2 \ll \nu^2 \\ i\,\dfrac{q}{p}\dfrac{k_1}{\nu}\dfrac{(1-\alpha)(1-\beta)}{(1+\alpha)(1+\beta)}\dfrac{A_{1T}}{A_{1S}} & \text{for } k_2^2 \gg \nu^2 \gg k_1^2 \end{cases} \qquad (3.31)$$

Consequently, unless $\left|\frac{k_1}{k_2}\right|$ becomes comparable with k_2/ν (in usual cases $\left|\frac{k_1\nu}{k_2^2}\right| \ll 1$), the second type electric field may safely be ignored on condition that the intensity of the source field of both types (A_{1T} and A_{1S}) are of the same order of magnitude.

3–4. Successive approximation of the induction problem.

Although the rigorous solutions have already been obtained for electromagnetic induction in horizontally stratified structures, a method of successive approximation is discussed in this section. A similar method will then be employed for the study of a tilted boundary.

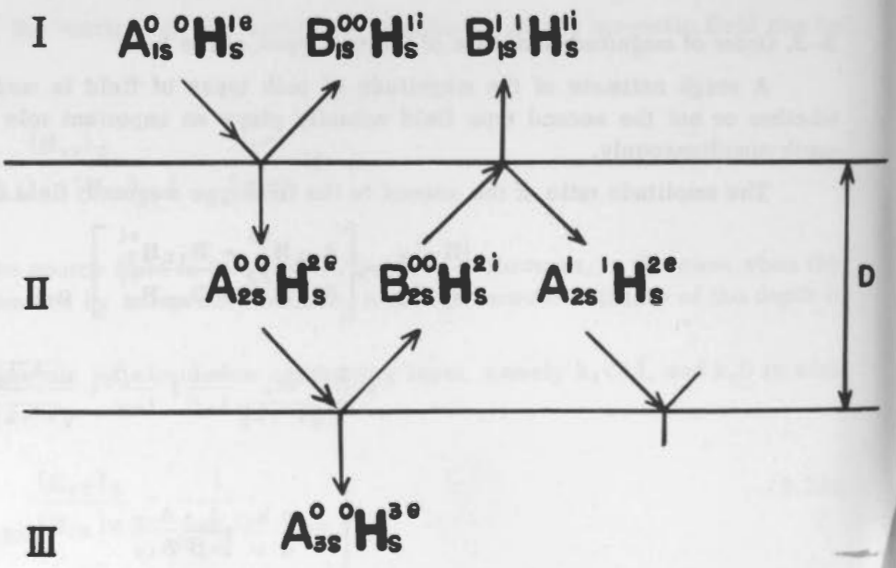

FIGURE 2. Illustration of successive approximation for a horizontal structure model.

Suppose the first type field $A_{1S}^{0}\,{}^{0}H_S^{1e}$ is applied to the earth as in Figure 2. A part of the energy will be reflected back into the atmosphere as $B_{1S}^{0}\,{}^{0}H_S^{1i}$, and the other part of the energy will be transmitted into the II layer ($A_{2S}^{0}\,{}^{0}H_S^{2e}$).

When $A^0_{2S}\,{}^0\mathbf{H}^{2e}_S$ field arrives at the other boundary (II–III), energy will be partly reflected ($B^0_{2S}\,{}^0\mathbf{H}^{2i}_S$) and partly transmitted ($A^0_{3S}\,{}^0\mathbf{H}^{3e}_S$). The reflected field $B^0_{2S}\,{}^0\mathbf{H}^{2i}_S$ will repeat the same kind of reflection and transmission at the ground surface (II–I). Repeating the same procedure, we have a series of reflected field $B^0_{1S}\,{}^0\mathbf{H}^{1i}_S$, $B^1_{1S}\,{}^1\mathbf{H}^{1i}_S$, $B^2_{1S}\,{}^2\mathbf{H}^{1i}_S$, ... in the I layer. And we can approximate the magnetic field in the atmosphere by the following series.

$$\left.\begin{aligned}\mathbf{H} &= A^0_{1S}\,{}^0\mathbf{H}^{1e}_S + B^0_{1S}\,{}^0\mathbf{H}^{1i}_S + B^1_{1S}\,{}^1\mathbf{H}^{1i}_S + \cdots \\ &= A^0_{1S}\,{}^0\mathbf{H}^{1e}_S + B_{1S}\mathbf{H}^{1i}_S\end{aligned}\right\} \quad (3.32)$$

$$\text{where } B_{1S} = B^0_{1S} + B^1_{1S} + \cdots \quad (3.33)$$

The above series may be expected to converge rapidly if the attenuation of the field due to diffusion is quite rapid within the layer II or if the energy which should be stored within the layer II is significantly diminished at every reflection at the boundary.

In the first place, the boundary conditions should be satisfied for the electromagnetic fields specified by I–II boundary, $A^0_{1S}\,{}^0\mathbf{H}^{1e}_S$, $B^0_{1S}\,{}^0\mathbf{H}^{1i}_S$, $A^0_{2S}\,{}^0\mathbf{H}^{2e}_S$, $A^0_{1S}\,{}^0\mathbf{E}^{1e}_T$, $B^0_{1S}\,{}^0\mathbf{E}^{1i}_T$, $A^0_{2S}\,{}^0\mathbf{E}^{2e}_T$.
Then we have

$$\left.\begin{aligned}B^0_{1S} &= \frac{\sqrt{\nu^2+k_1^2}-\sqrt{\nu^2+k_2^2}}{\sqrt{\nu^2+k_1^2}+\sqrt{\nu^2+k_2^2}}\,A^0_{1S} \\ A^0_{2S} &= \frac{k_2}{k_1}\,\frac{2\sqrt{\nu^2+k_1^2}}{\sqrt{\nu^2+k_1^2}+\sqrt{\nu^2+k_2^2}}\,A^0_{1S}\end{aligned}\right\} \quad (3.34)$$

Secondly, the coefficients A^0_{3S} and B^0_{2S} can be calculated with reference to the known quantity A^0_{2S}.

$$\left.\begin{aligned}B^0_{2S} &= \frac{\sqrt{\nu^2+k_2^2}-\sqrt{\nu^2+k_3^2}}{\sqrt{\nu^2+k_2^2}+\sqrt{\nu^2+k_3^2}}\,e^{-\sqrt{\nu^2+k_2^2}D}\,A^0_{2S} \\ A^0_{3S} &= \frac{k_3}{k_2}\,\frac{2\sqrt{\nu^2+k_2^2}}{\sqrt{\nu^2+k_2^2}+\sqrt{\nu^2+k_3^2}}\,e^{-\sqrt{\nu^2+k_2^2}D}\,A^0_{2S}\end{aligned}\right\} \quad (3.35)$$

A similar procedure enables us to calculate the coefficients B^1_{1S} and A^1_{2S}.

$$\left.\begin{aligned}A^1_{2S} &= \frac{\sqrt{\nu^2+k_2^2}-\sqrt{\nu^2+k_1^2}}{\sqrt{\nu^2+k_2^2}+\sqrt{\nu^2+k_1^2}}\,e^{-\sqrt{\nu^2+k_2^2}D}\,B^0_{2S} \\ B^1_{1S} &= \frac{k_1}{k_2}\,\frac{2\sqrt{\nu^2+k_2^2}}{\sqrt{\nu^2+k_2^2}+\sqrt{\nu^2+k_1^2}}\,e^{-\sqrt{\nu^2+k_2^2}D}\,B^0_{2S}\end{aligned}\right\} \quad (3.36)$$

On the other hand, the coefficient B_{1S} in (3.34) has already been obtained rigorously in the case of horizontally stratified structure in the equation (3.17). It can be rewritten as follows,

$$B_{1S} = \frac{\sqrt{\nu^2+k_1^2}-\sqrt{\nu^2+k_2^2}}{\sqrt{\nu^2+k_1^2}+\sqrt{\nu^2+k_2^2}} \frac{1+\dfrac{\sqrt{\nu^2+k_1^2}+\sqrt{\nu^2+k_2^2}}{\sqrt{\nu^2+k_1^2}-\sqrt{\nu^2+k_2^2}}\beta}{1-\dfrac{\sqrt{\nu^2+k_1^2}-\sqrt{\nu^2+k_2^2}}{\sqrt{\nu^2+k_1^2}+\sqrt{\nu^2+k_2^2}}\beta} A_{1S}^0 \qquad (3.37)$$

When either β or $\dfrac{\sqrt{\nu^2+k_1^2}-\sqrt{\nu^2+k_2^2}}{\sqrt{\nu^2+k_1^2}+\sqrt{\nu^2+k_2^2}}$ is small, the above equation can be written as follows,

$$\begin{aligned} B_{1S} &= \beta\left\{1-\frac{\sqrt{\nu^2+k_1^2}-\sqrt{\nu^2+k_2^2}}{\sqrt{\nu^2+k_1^2}+\sqrt{\nu^2+k_2^2}}\left(\beta-\frac{1}{\beta}\right)+\left(\frac{\sqrt{\nu^2+k_1^2}-\sqrt{\nu^2+k_2^2}}{\sqrt{\nu^2+k_1^2}+\sqrt{\nu^2+k_2^2}}\right)^2+\cdots\right\} A_{1S}^0 \\ &= \left[\frac{\sqrt{\nu^2+k_1^2}-\sqrt{\nu^2+k_2^2}}{\sqrt{\nu^2+k_1^2}+\sqrt{\nu^2+k_2^2}}+\frac{4\sqrt{\nu^2+k_1^2}\sqrt{\nu^2+k_2^2}}{(\sqrt{\nu^2+k_1^2}+\sqrt{\nu^2+k_2^2})^2}\beta-\frac{\sqrt{\nu^2+k_1^2}-\sqrt{\nu^2+k_2^2}}{\sqrt{\nu^2+k_1^2}+\sqrt{\nu^2+k_2^2}}\beta^2+\cdots\right] A_{1S} \end{aligned} \qquad (3.38)$$

Comparing the above equation with B_{1S}^0 and B_{1S}^1 in the equations (3.34), (3.36), it can easily be seen that the first term corresponds to B_{1S}^0 and the second to B_{1S}^1. Therefore the equation (3.38) is identical with the expression (3.33).

The requirement for β being small is satisfied when:

1) $e^{-2\sqrt{\nu^2+k_2^2}D}$ is small; this means that the field attenuation due to diffusion is large. This occurs when the conductivity of the II layer is high enough;

2) $\dfrac{\sqrt{\nu^2+k_2^2}-\sqrt{\nu^2+k_3^2}}{\sqrt{\nu^2+k_2^2}+\sqrt{\nu^2+k_3^2}}$ is small; this means that only a small portion of the energy is reflected back to the II layer owing to the small difference in electrical conductivity between the II and III layer.

$\dfrac{\sqrt{\nu^2+k_1^2}-\sqrt{\nu^2+k_2^2}}{\sqrt{\nu^2+k_1^2}+\sqrt{\nu^2+k_2^2}}$ becomes small when either (a) k_1 and k_2 are small compared with ν (this condition may usually be satisfied when both I and II layers have such poor conductivity as 10^{-15} emu.), or (b) k_1 and k_2 are similar.

So long as the above conditions are satisfied, it may be concluded that the induction problem for the first type field can be approximated by the successive approximation procedure described in this section.

4. Electromagnetic Induction at a Tilted Boundary

Within the second layer II (Figure 3), the second type field H_{2T}^0 has no Z component of the magnetic field in the coordinate system of (X, Y, Z). In the tilted coordinates (X′, Y′, Z′), however, it is expressed by a synthesized field of both types, the first type (having Z′ component) and the second type field (without Z′ component).

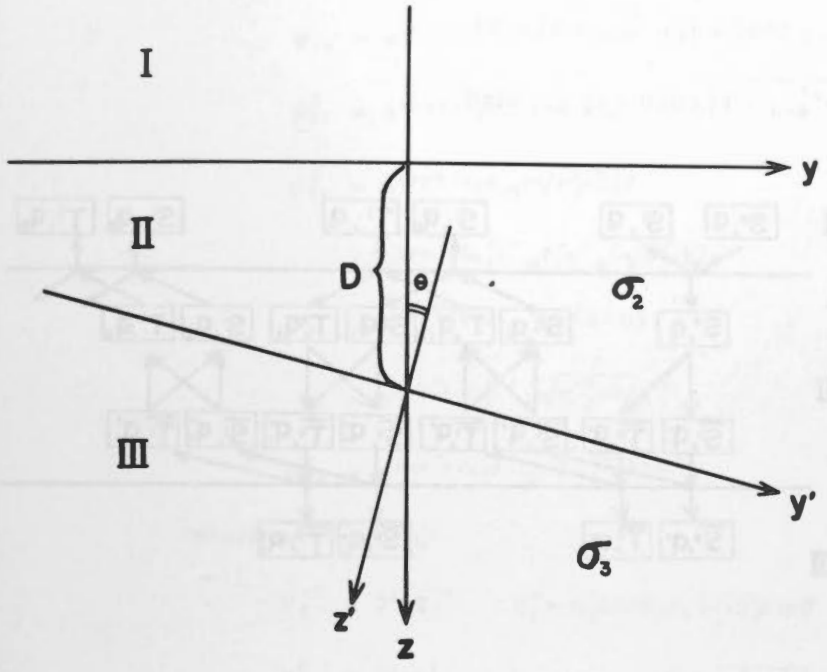

FIGURE 3. Earth model with an inclined interface.

Consequently one of the characteristic features of the tilted boundary problem is the splitting of the field into two different types that takes place at the boundary. When the first type field is applied from outside the earth, and arrives at the tilted boundary, it will then be split into the first and second type fields and will be reflected back to the ground surface. At the ground surface it will be split into both types again and reflected downwards. This procedure is supposedly repeated in layer II.

The other characteristic feature is the modification of wave numbers. As will be discussed later, the source field can be represented, in general, as a sum of elementary harmonics of the form $e^{ipx+iqy+rz}$, where $r=-\sqrt{\nu^2+k_j^2}$. Such elementary fields may be transformed into $e^{ip'x'+iq'y'+r'z'}$ in the tilted coordinates (X', Y', Z') where $p'=p$, $q'=\cos\theta+i\sqrt{\nu^2+k_2^2}\sin\theta$ and $r'=-\sqrt{\nu^2+k_2^2}\cos\theta - iq\sin\theta$. This indicates that an elongation of the wave length in the y-direction (by a factor of $1/\cos\theta$) takes place at every reflection and that the field attenuates in the y'-direction. In this study, however, the discussion is limited to small angles of tilt which satisfy the condition $\tan\theta \ll \frac{q}{\sqrt{\nu^2+k_2^2}}$, where attenuation in the y'-direction is small and the electromagnetic field can be approximated by superposition of harmonic functions only.

The above procedures are schematically shown in Figure 4, where S^e and S^i designate the first type field of external and internal origin respectively. T^e and T^i represent the second type field of external and internal origin. S and T are the fields expressed in the coordinate system (X, Y, Z), while $\overline{S}$, $\overline{T}$ are those in (X', Y', Z') coordinates. Other quantities in the figures are defined as follows,

$$\nu_s'^2 = p^2 + q_s'^2$$

$$q_s' = q_s\cos\theta + i\sqrt{\nu_s^2 + k_2^2}\sin\theta$$

$$r_s' = -\sqrt{\nu_s^2 + k_2^2}\cos\theta - iq_s\sin\theta$$

$$\nu_s^2 = p^2 + q_s^2$$

$$q_S = q'_{S-1}\cos\theta + i\sqrt{\nu'^2_{S-1} + k_z^2}\sin\theta$$

$$r_S = \sqrt{\nu'^2_{S-1} + k_z^2}\cos\theta + iq'_{S-1}\sin\theta$$

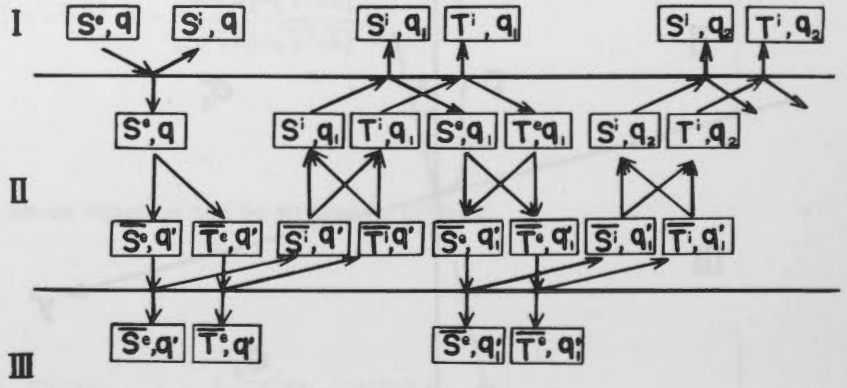

FIGURE 4. Production of two different types of the field and modification of wave numbers at the boundaries in the case of the first type field being applied. S represents the first type field and T the second type field. $\bar{S}$ is the first type field expressed in (x′, y′, z′) coordinates, whereas S is the field in (x, y, z) coordinates. The arrows designate the direction of energy flow.

4–2. Mathematical expression of the field

The first and the second type field in the j–th layer can be written in the (X, Y, Z) coordinates as follows,

$$\left.\begin{aligned}
{}^{l}\mathbf{H}^{j}_{S} &= \frac{1}{ik_j}\begin{bmatrix} \dfrac{\partial^2\psi^l_j}{\partial x\partial z} \\ \dfrac{\partial^2\psi^l_j}{\partial y\partial z} \\ -\dfrac{\partial^2\psi^l_j}{\partial x^2} - \dfrac{\partial^2\psi^l_j}{\partial z^2} \end{bmatrix} \qquad {}^{l}\mathbf{E}^{j}_{T} = -\frac{\omega\mu}{k_j}\begin{bmatrix} \dfrac{\partial\psi^l_j}{\partial y} \\ -\dfrac{\partial\psi^l_j}{\partial x} \\ 0 \end{bmatrix} \\
{}^{l}\mathbf{H}^{j}_{T} &= \begin{bmatrix} \dfrac{\partial\psi^l_j}{\partial y} \\ -\dfrac{\partial\psi^l_j}{\partial x} \\ 0 \end{bmatrix} \qquad {}^{l}\mathbf{E}^{j}_{S} = \frac{i\omega\mu}{k_j^2}\begin{bmatrix} \dfrac{\partial^2\psi^l_j}{\partial x\partial z} \\ \dfrac{\partial^2\psi^l_j}{\partial y\partial z} \\ -\dfrac{\partial^2\psi^l_j}{\partial x^2} - \dfrac{\partial^2\psi^l_j}{\partial y^2} \end{bmatrix}
\end{aligned}\right\} \quad (4.2.1)$$

where ψ_j is a function that should satisfy the following equation, $\Delta^2\psi_j + k_j^2\psi_j = 0$. The fields $\bar{\mathbf{H}}_S$, $\bar{\mathbf{E}}_T$, $\bar{\mathbf{H}}_T$, $\bar{\mathbf{E}}_S$ in the (X′, Y′, Z′) coordinates are obtained by differentiating ψ_j with respect to x′, y′ and z′ in place of x, y and z in (4.2.1).

The function ψ_j satisfying the preceding relation can be obtained as follows,

$$\psi_{1e} = e^{ipx+iqy}\, e^{-\sqrt{\nu^2+k_1^2}z}$$

$$\psi_{1i}^{l} = e^{ipx+iq_l y}\, e^{\sqrt{\nu^2+k_1^2}z}$$

$$\psi_{2e}^{l} = e^{ipx+iq_l y}\, e^{-\sqrt{\nu_l^2+k_2^2}z}$$

$$= e^{ipx'+iq_l' y'}\, e^{r_l' z'}\, e^{-\sqrt{\nu_l^2+k_2^2}D}$$

$$\psi_{2i}^{l} = e^{ipx+iq_l y}\, e^{r_{l+1}(z-D)}$$

$$= e^{ipx'+iq_l' y'}\, e^{\sqrt{\nu_l'^2+k_2^2}z'}$$

$$\psi_{3e}^{l} = e^{ipx'+iq_l' y'}\, e^{-\sqrt{\nu_l'^2+k_2^2}z'}$$

where $\nu^2 = p^2+q^2$

$$\nu_l'^2 = p^2+q_l'^2 \qquad q_l' = q_l\cos\theta+i\sqrt{\nu_l^2+k_2^2}\sin\theta \qquad r_l' = -\sqrt{\nu_l^2+k_2^2}\cos\theta-iq_l\sin\theta$$

$$\nu_l^2 = p^2+q_l^2 \qquad q_l = q_{l-1}\cos\theta+i\sqrt{\nu_{l-1}'^2+k_2^2}\sin\theta \qquad r_l = \sqrt{\nu_{l-1}'^2+k_2^2}\cos\theta+iq_{l-1}\sin\theta$$

$\psi_{j_e}^{l}$ and $\psi_{j_i}^{l}$ are the potential function of the external and internal origin in the j–the layer.

4–3. The first type field as an external field

In order to solve the electromagnetic induction problem at a tilted boundary, we will employ the successive approximation discussed in section 3–4. In this section, the electromagnetic induction when the first type field is applied to the tilted boundary model in Figure 3 is discussed in some detail.

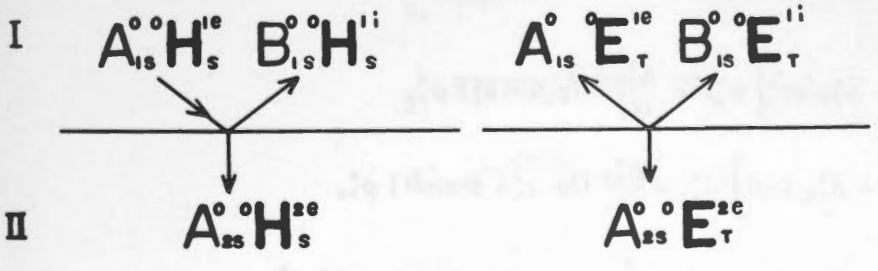

FIGURE 5. Procedure of successive approximation (the first stage).

At the ground surface (I–II), boundary conditions should be satisfied for the magnetic fields $A_{1S}^{0}\,{}^{0}H_S^{1e}$, $A_{2S}^{0}\,{}^{0}H_S^{2e}$, $B_{1S}^{0}\,{}^{0}H_S^{1i}$ and the electric fields $A_{1S}^{0}\,{}^{0}E_T^{1e}$, $A_{2S}^{0}\,{}^{0}E_T^{2e}$, $B_{1S}^{0}\,{}^{0}E_T^{1i}$ as is shown in Figure 5. Then the required conditions are reduced to the following two equations,

$$\frac{1}{k_1}\sqrt{\nu^2+k_1^2}\,(A_{1S}^{0}-B_{1S}^{0}) = \frac{1}{k_2}\sqrt{\nu^2+k_2^2}\,A_{2S}^{0}$$

$$\frac{1}{k_1}\,(A_{1S}^{0}+B_{1S}^{0}) = \frac{A_{2S}^{0}}{k_2}$$

From these, we obtain

$$B^0_{1S} = \frac{\sqrt{\nu^2+k_1^2}-\sqrt{\nu^2+k_2^2}}{\sqrt{\nu^2+k_1^2}+\sqrt{\nu^2+k_2^2}} A^0_{1S}$$

$$A^0_{2S} = \frac{k_2}{k_1} \frac{2\sqrt{\nu^2+k_1^2}}{\sqrt{\nu^2+k_1^2}+\sqrt{\nu^2+k_2^2}} A^0_{1S}$$

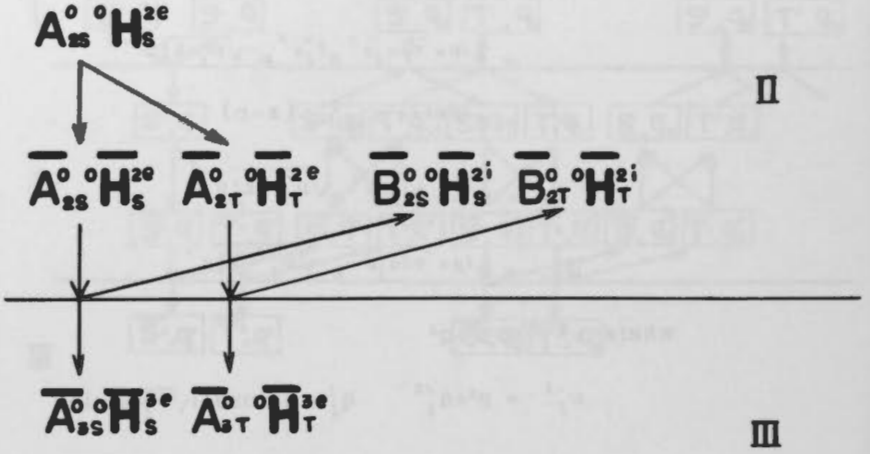

FIGURE 6. Procedure of successive approximation (the second stage).

Splitting of the first type field at the tilted boundary (II–III) is illustrated in Figure 6. As a matter of course, each component of the total field expressed in the tilted coordinates ($A^0_{2S}{}^0\bar{H}^{2e}_S + A^0_{2T}\bar{H}^{2e}_T$) should be identical with that of the incident field ($\bar{A}^0_{2S}{}^0\bar{H}^{2e}_S$). Thus the following relations should be satisfied.

$$\left[\bar{A}^0_{2S}{}^0\bar{H}^{2e}_S + \bar{A}^0_{2T}{}^0\bar{H}^{2e}_T\right]_x = \left[A^0_{2S}{}^0H^{2e}_S\right]_x$$

$$\left[\bar{A}^0_{2S}{}^0\bar{H}^{2e}_S + \bar{A}^0_{2T}{}^0\bar{H}^{2e}_T\right]_y = \left[A^0_{2S}{}^0H^{2e}_S\right]_y\cos\theta + \left[A^0_{2S}{}^0H^{2e}_S\right]_z\sin\theta$$

$$\left[\bar{A}^0_{2S}{}^0\bar{H}^{2e}_S + \bar{A}^0_{2T}{}^0\bar{H}^{2e}_T\right]_z = -\left[A^0_{2S}{}^0H^{2e}_S\right]_y\sin\theta + \left[A^0_{2S}{}^0H^{2e}_S\right]_z\cos\theta$$

These are written explicitly as follows,

$$\left[\bar{A}^0_{2S}\frac{1}{ik_2}(ip)\,r' + \bar{A}^0_{2T}\,iq'\right]\psi^0_{2e} = \frac{A^0_{2S}}{ik_2}\left[-ip\sqrt{\nu^2+k_2^2}\right]\psi^0_{2e}$$

$$\left[\bar{A}^0_{2S}\frac{1}{ik_2}(iq')\,r' - \bar{A}^0_{2T}(ip)\right]\psi^0_{2e} = \frac{A^0_{2S}}{ik_2}\left[iq\cdot r' + p^2\sin\theta\right]\psi^0_{2e}$$

$$\bar{A}^0_{2S}\frac{1}{ik_2}\nu'^2\psi^0_{2e} = \frac{A^0_{2S}}{ik_2}\left[(-iq)(iq') + p^2\cos\theta\right]\psi^0_{2e}$$

In the same way we have the following equations for the electric field,

$$\left[\bar{A}^0_{2S}\frac{\omega\mu}{k_2}iq' - \bar{A}^0_{2T}\frac{i\omega\mu}{k_2^2}(ip\cdot r')\right]\psi^0_{2e} = A^0_{2S}\frac{\omega\mu}{k_2}(iq)\,\psi^0_{2e}$$

$$\left[\bar{A}^0_{2S}\frac{\omega\mu}{k_2}(-ip) - \bar{A}^0_{2T}\frac{i\omega\mu}{k_2^2}(iq'\cdot r')\right]\psi^0_{2e} = A^0_{2S}\frac{\omega\mu}{k_2}(-ip\cos\theta)\,\psi^0_{2e}$$

$$-\bar{A}^0_{2T}\frac{i\omega\mu}{k_2^2}\nu'^2\psi^0_{2e} = A^0_{2S}\frac{\omega\mu}{k_2}(ip\sin\theta)\,\psi^0_{2e}$$

These give the following relationship between A^0_{2S}, A^{-0}_{2S} and A^{-0}_{2T}.

$$\bar{A}^0_{2S} = \frac{(-iq)\, iq' + p^2\cos\theta}{\nu'^2} A^0_{2S}$$

$$\bar{A}^0_{2T} = ik_2 \frac{ip\sin\theta}{\nu'^2} A^0_{2S}$$

Then the boundary conditions can be written as follows,

$$ip\left[\frac{1}{ik_2}\{\bar{A}^0_{2S} r' e^{-\sqrt{\nu^2+k_2^2}D} + \bar{B}^0_{2S}\sqrt{\nu'^2+k_2^2}\} + \frac{1}{ik_3}\bar{A}^0_{3S}\sqrt{\nu'^2+k_3^2}\right] + iq'\left[\bar{A}^0_{2T} e^{-\sqrt{\nu^2+k_2^2}D} + \bar{B}^0_{2T} - \bar{A}^0_{3T}\right] = 0$$

$$ip'\left[\frac{1}{ik_2}\{\bar{A}^0_{2S} r' e^{-\sqrt{\nu^2+k_2^2}D} + \bar{B}^0_{2S}\sqrt{\nu'^2+k_2^2}\} + \frac{1}{ik_3}\bar{A}^0_{3S}\sqrt{\nu'^2+k_3^2}\right] - ip\left[\bar{A}^0_{2T} e^{-\sqrt{\nu^2+k_2^2}D} + \bar{B}^0_{2T} - \bar{A}^0_{3T}\right] = 0$$

$$\frac{1}{k_2}\{\bar{A}^0_{2S} e^{-\sqrt{\nu^2+k_2^2}D} + \bar{B}^0_{2S}\} - \frac{1}{k_3}\bar{A}^0_{3S} = 0$$

for the magnetic field; and

$$i\omega\mu(iq')\left[\frac{1}{ik_2}\{\bar{A}^0_{2S} e^{-\sqrt{\nu^2+k_2^2}D} + \bar{B}^0_{2S}\} - \frac{1}{ik_3}\bar{A}^0_{3S}\right] + i\omega\mu(ip)\left[\frac{1}{k_2^2}\{\bar{A}^0_{2T} r' e^{-\sqrt{\nu^2+k_2^2}D} + \bar{B}^0_{2T}\sqrt{\nu'^2+k_2^2}\} + \frac{1}{k_3^2}\bar{A}^0_{3T}\sqrt{\nu'^2+k_2^2}\right] = 0$$

$$i\omega\mu(-ip)\left[\frac{1}{ik_2}\{\bar{A}^0_{2S} e^{-\sqrt{\nu^2+k_2^2}D} + \bar{B}^0_{2S}\} - \frac{1}{ik_3}\bar{A}^0_{3S}\right] + i\omega\mu(iq')\left[\frac{1}{k_2^2}\{\bar{A}^0_{2T} r' e^{-\sqrt{\nu^2+k_2^2}D} + \bar{B}^0_{2T}\sqrt{\nu'^2+k_2^2}\} + \frac{1}{k_3^2}\bar{A}^0_{3T}\sqrt{\nu'^2+k_2^2}\right] = 0$$

for the electric field.

Since p and q′ vary independently, the above equations can be separated and simplified as follows,

$$\frac{1}{k_2}\left[\bar{A}^0_{2S} r' e^{-\sqrt{\nu^2+k_2^2}D} + \bar{B}^0_{2S}\sqrt{\nu'^2+k_2^2}\right] = -\frac{1}{k_3}\bar{A}^0_{3S}\sqrt{\nu'^2+k_3^2}$$

$$\frac{1}{k_2}\left[\bar{A}^0_{2S} e^{-\sqrt{\nu^2+k_2^2}D} + \bar{B}^0_{2S}\right] = \frac{1}{k_3}\bar{A}^0_{3S}$$

$$\bar{A}^0_{2T} e^{-\sqrt{\nu^2+k_2^2}D} + \bar{B}^0_{2T} = \bar{A}^0_{3T}$$

$$\bar{A}^0_{2T} r' e^{-\sqrt{\nu^2+k_2^2}D} + \bar{B}^0_{2T}\sqrt{\nu'^2+k_2^2} = -\frac{k_2^2}{k_3^2}\bar{A}^0_{3T}\sqrt{\nu'^2+k_3^2}$$

The separation of the equations shown above indicates that the first (S) and the second (T) type field should satisfy the boundary conditions independently.

Solving these, we have

$$\bar{B}^0_{2S} = -\frac{r' + \sqrt{\nu'^2+k_3^2}}{\sqrt{\nu'^2+k_2^2} + \sqrt{\nu'^2+k_3^2}} e^{-\sqrt{\nu^2+k_2^2}D} \bar{A}^0_{2S}$$

$$\bar{A}^0_{3S} = -\frac{k_3}{k_2}\frac{r' - \sqrt{\nu'^2+k_2^2}}{\sqrt{\nu'^2+k_2^2} + \sqrt{\nu'^2+k_3^2}} e^{-\sqrt{\nu^2+k_2^2}D} \bar{A}^0_{2S}$$

$$\bar{B}^0_{2T} = -\frac{r' + \frac{k_2^2}{k_3^2}\sqrt{\nu'^2+k_3^2}}{\sqrt{\nu'^2+k_2^2} + \frac{k_2^2}{k_3^2}\sqrt{\nu'^2+k_3^2}} e^{-\sqrt{\nu^2+k_3^2}D}\ \bar{A}^0_{2T}$$

$$\bar{A}^0_{3T} = -\frac{r' - \sqrt{\nu'^2+k_2^2}}{\sqrt{\nu'^2+k_2^2} + \frac{k_2^2}{k_3^2}\sqrt{\nu'^2+k_3^2}} e^{-\sqrt{\nu^2+k_3^2}D}\ \bar{A}^0_{2T}$$

When the reflected energy of the first type field ($B^0_{2S}{}^0H^{2i}_S$) arrives at the ground surface (I–II), it will be split into the two types $B^0_{2S}{}^0H^{2i}_S$ and $B^0_{2T}{}^0H^{2i}_T$. Then a part of the energy will be transmitted into the air in the forms of $B^1_{1S}{}^1H^{1i}_S$ and $B^1_{1T}{}^1H^{1i}_T$, and the other part of the energy will be reflected back into the earth as $A^2_{2S}{}^1H^{2e}_S$, $A^1_{2T}{}^1H^{2e}_T$ (Figure 7).

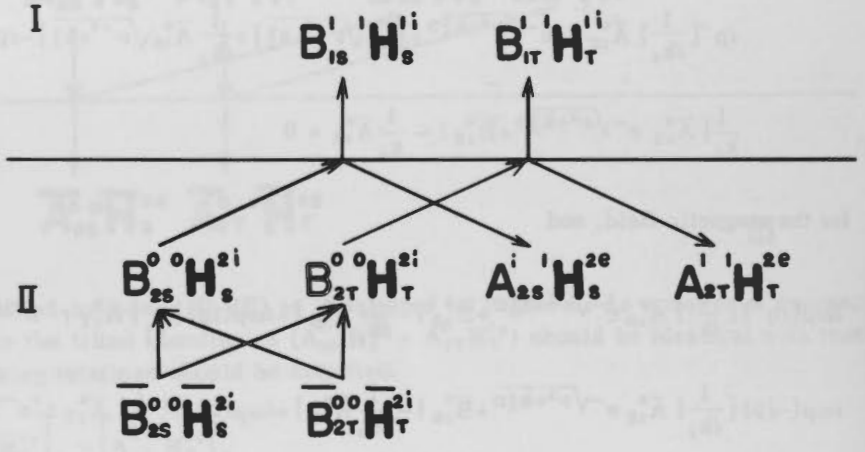

FIGURE 7. Procedure of successive approximation (the third stage).

In this case, the split of the field may be formulated as follows,

$$\bar{B}^0_{2S} = \frac{1}{\nu_1^2}\left[\bar{B}^0_{2S}\{(-iq')(iq_1) + p^2\cos\theta\} + \bar{B}^0_{2T}\, ik_2(-ip)\sin\theta\right]$$

$$\bar{B}^0_{2T} = \frac{1}{\nu_1^2}\left[\bar{B}^0_{2S}\, ik_2(-ip\sin\theta) + \bar{B}^0_{2T}\{(-iq')\cdot(iq_1) + p^2\cos\theta\}\right]$$

And the boundary conditions at $z = 0$ are written,

a) for the first type field,

$$\frac{1}{k_2}\left[B^0_{2S} r_1 e^{-r_1 D} - A^1_{2S}\sqrt{\nu_1^2+k_2^2}\right] = \frac{1}{k_1}$$

$$\frac{1}{k_2}\left[B^0_{2S} e^{-r_1 D} + A^1_{2S}\right] = \frac{1}{k_1} B^1_{1S}$$

b) for the second type field,

$$B^0_{2T} e^{-r_1 D} + A^1_{2T} = B^1_{1T}$$

$$B^0_{2T} r_1 e^{-r_1 D} - A^1_{2T}\sqrt{\nu_1^2+k_2^2} = \frac{k_2^2}{k_3^2} B^1_{1T}\sqrt{\nu_1^2+k_1^2}$$

Thus we obtain

$$A^1_{2S} = \frac{r_1 - \sqrt{\nu_1^2+k_1^2}}{\sqrt{\nu_1^2+k_2^2}+\sqrt{\nu_1^2+k_1^2}} e^{-r_1 D} B^0_{2S}$$

$$B^1_{1S} = \frac{k_1}{k_2}\frac{r_1 + \sqrt{\nu_1^2+k_2^2}}{\sqrt{\nu_1^2+k_2^2}+\sqrt{\nu_1^2+k_1^2}} e^{-r_1 D} B^0_{2S}$$

$$A^1_{2T} = \frac{r_1 - \frac{k_2^2}{k_1^2}\sqrt{\nu_1^2+k_1^2}}{\sqrt{\nu_1^2+k_2^2}+\frac{k_2^2}{k_1^2}\sqrt{\nu_1^2+k_1^2}} e^{-r_1 D} B^0_{2T}$$

$$B^1_{1T} = \frac{r_1 + \sqrt{\nu_1^2+k_2^2}}{\sqrt{\nu_1^2+k_2^2}+\frac{k_2^2}{k_1^2}\sqrt{\nu_1^2+k_1^2}} e^{-r_1 D} B^0_{2T}$$

Repeating the same procedures between the two boundaries, we can calulate the coefficients B^l_{1S}, A^l_{2S}, $\bar{A}^l_{2S}$, $\bar{A}^l_{2T}$, $\bar{B}^l_{2S}$, $\bar{B}^l_{2T}$, $\bar{A}^l_{3S}$, $\bar{A}^l_{3T}$, B^l_{2S}, B^l_{2T} (l= 1, 2, 3, ...) sucessively.

These solutions are summarized as follows:

$$\left.\begin{aligned} B^0_{1S} &= \frac{\sqrt{\nu^2+k_1^2}-\sqrt{\nu^2+k_2^2}}{\sqrt{\nu^2+k_1^2}+\sqrt{\nu^2+k_2^2}} A^0_{1S} \\ A^0_{2S} &= \frac{k_2}{k_1}\frac{2\sqrt{\nu^2+k_1^2}}{\sqrt{\nu^2+k_1^2}+\sqrt{\nu^2+k_2^2}} A^0_{1S} \end{aligned}\right\} \quad (4.3.1)$$

$$\left.\begin{aligned} \bar{A}^0_{2S} &= \frac{1}{\nu'_2}[\,(-iq)(iq') + p^2\cos\theta\,]\, A^0_{2S} \\ \bar{A}^0_{2T} &= \frac{i}{\nu'_2} k_2(ip)\sin\theta\, A^0_{2S} \end{aligned}\right\} \quad (4.3.2)$$

$$\left.\begin{aligned} \bar{B}^0_{2S} &= -\frac{r' + \sqrt{\nu'^2+k_3^2}}{\sqrt{\nu'^2+k_2^2}+\sqrt{\nu'^2+k_3^2}} e^{-\sqrt{\nu^2+k_2^2}D} \bar{A}^0_{2S} \\ \bar{A}^0_{3S} &= -\frac{k_3}{k_2}\frac{r' + \sqrt{\nu'^2+k_2^2}}{\sqrt{\nu'^2+k_2^2}+\sqrt{\nu'^2+k_3^2}} e^{-\sqrt{\nu^2+k_2^2}D} \bar{A}^0_{2S} \\ \bar{B}^0_{2T} &= -\frac{r' + \frac{k_2^2}{k_3^2}\sqrt{\nu'^2+k_3^2}}{\sqrt{\nu'^2+k_2^2}+\frac{k_2^2}{k_3^2}\sqrt{\nu'^2+k_3^2}} e^{-\sqrt{\nu^2+k_2^2}D} \bar{A}^0_{2T} \\ \bar{A}^0_{3T} &= -\frac{r' - \sqrt{\nu'^2+k_2^2}}{\sqrt{\nu'^2+k_2^2}+\frac{k_2^2}{k_3^2}\sqrt{\nu'^2+k_3^2}} e^{-\sqrt{\nu^2+k_2^2}D} \bar{A}^0_{2T} \end{aligned}\right\} \quad (4.3.3)$$

$$\left.\begin{aligned} B^0_{2S} &= \frac{1}{\nu_1^2}[\,\bar{B}^0_{2S}\{(-iq')(iq_1)+p^2\cos\theta\}+\bar{B}^0_{2T}(ik_2)(-ip)\sin\theta\,] \\ B^0_{2T} &= \frac{1}{\nu_1^2}[\,\bar{B}^0_{2S}(ik_2)(-ip\sin\theta)+\bar{B}^0_{2T}\{(-iq')(iq_1)+p^2\cos\theta\}\,] \end{aligned}\right\} \quad (4.3.4)$$

$$
\left.
\begin{aligned}
A^1_{2S} &= \frac{r_1 - \sqrt{\nu_1^2+k_1^2}}{\sqrt{\nu_1^2+k_2^2}+\sqrt{\nu_1^2+k_1^2}}\, e^{-r_1 D}\, B^0_{2S} \\
B^1_{1S} &= \frac{k_1}{k_2}\,\frac{r_1+\sqrt{\nu_1^2+k_2^2}}{\sqrt{\nu_1^2+k_2^2}+\sqrt{\nu_1^2+k_1^2}}\, e^{-r_1 D}\, B^0_{2S} \\
B^1_{1T} &= \frac{r_1+\sqrt{\nu_1^2+k_2^2}}{\sqrt{\nu_1^2+k_2^2}+\frac{k_2^2}{k_1^2}\sqrt{\nu_1^2+k_1^2}}\, e^{-r_1 D}\, B^0_{2T} \\
A^1_{2T} &= \frac{r_1 - \frac{k_2^2}{k_1^2}\sqrt{\nu_1^2+k_1^2}}{\sqrt{\nu_1^2+k_2^2}+\frac{k_2^2}{k_1^2}\sqrt{\nu_1^2+k_1^2}}\, e^{-r_1 D}\, B^0_{2T}
\end{aligned}
\right\} \quad (4.3.5)
$$

$$
\left.
\begin{aligned}
\bar{A}^1_{2S} &= \frac{1}{\nu_1'^2}\left[\, A^1_{2S}\{(-iq_1')(iq_1)+p^2\cos\theta\}+A^1_{2T}(ik_2)(ip)\sin\theta\,\right] \\
\bar{A}^1_{2T} &= \frac{1}{\nu_1'^2}\left[\, A^1_{2S}(ik_2)(ip)\sin\theta+A^1_{2T}\{(-iq_1')(iq_1)+p^2\cos\theta\}\,\right]
\end{aligned}
\right\} \quad (4.3.6)
$$

$$
\left.
\begin{aligned}
\bar{B}^1_{2S} &= -\frac{r_1'+\sqrt{\nu_1'^2+k_3^2}}{\sqrt{\nu_1'^2+k_2^2}+\sqrt{\nu_1'^2+k_3^2}}\, e^{-\sqrt{\nu_1^2+k_2^2}D}\, \bar{A}^1_{2S} \\
\bar{A}^1_{3S} &= -\frac{k_3}{k_2}\,\frac{r_1'+\sqrt{\nu_1'^2+k_3^2}}{\sqrt{\nu_1'^2+k_2^2}+\sqrt{\nu_1'^2+k_3^2}}\, e^{-\sqrt{\nu_1^2+k_2^2}D}\, \bar{A}^1_{2S} \\
\bar{B}^1_{2T} &= -\frac{r_1'+\frac{k_2^2}{k_3^2}\sqrt{\nu_1'^2+k_3^2}}{\sqrt{\nu_1'^2+k_2^2}+\frac{k_2^2}{k_3^2}\sqrt{\nu_1'^2+k_3^2}}\, e^{-\sqrt{\nu_1^2+k_2^2}D}\, \bar{A}^1_{2T} \\
\bar{A}^1_{3T} &= -\frac{r_1'+\sqrt{\nu_1'^2+k_2^2}}{\sqrt{\nu_1'^2+k_2^2}+\frac{k_2^2}{k_3^2}\sqrt{\nu_1'^2+k_3^2}}\, e^{-\sqrt{\nu_1^2+k_2^2}D}\, \bar{A}^1_{2T}
\end{aligned}
\right\} \quad (4.3.7)
$$

$$
\left.
\begin{aligned}
B^1_{2S} &= \frac{1}{\nu_2^2}\left[\, \bar{B}^1_{2S}\{(-iq_1')(iq_2)+p^2\cos\theta\}+\bar{B}^1_{2T}(ik_2)(-ip)\sin\theta\,\right] \\
B^1_{2T} &= \frac{1}{\nu_2^2}\left[\, \bar{B}^1_{2S}(ik_2)(-ip\sin\theta)+\bar{B}^1_{2T}\{(-iq_1')(iq_2)+p^2\cos\theta\}\,\right]
\end{aligned}
\right\} \quad (4.3.8)
$$

$$
\left.
\begin{aligned}
B^2_{1S} &= \frac{k_1}{k_2}\frac{r_2+\sqrt{\nu_2^2+k_2^2}}{\sqrt{\nu_2^2+k_1^2}+\sqrt{\nu_2^2+k_2^2}}\,e^{-r_2 D}\,B^1_{2S}\\
A^2_{1S} &= \frac{r_2-\sqrt{\nu_2^2+k_1^2}}{\sqrt{\nu_2^2+k_1^2}+\sqrt{\nu_2^2+k_2^2}}\,e^{-r_2 D}\,B^1_{2S}\\
B^2_{1T} &= \frac{r_2+\sqrt{\nu_2^2+k_2^2}}{\sqrt{\nu_2^2+k_2^2}+\frac{k_2^2}{k_1^2}\sqrt{\nu_2^2+k_1^2}}\,e^{-r_2 D}\,B^1_{2T}\\
A^2_{1T} &= \frac{r_2-\frac{k_2^2}{k_1^2}\sqrt{\nu_2^2+k_1^2}}{\sqrt{\nu_2^2+k_2^2}+\frac{k_2^2}{k_1^2}\sqrt{\nu_2^2+k_1^2}}\,e^{-r_2 D}\,B^1_{2T}\\
&\text{- - - - - - -}\\
&\text{- - - - - - -}
\end{aligned}
\right\} \quad (4.3.9)
$$

$$
\left.
\begin{aligned}
\bar{A}^l_{2S} &= \frac{1}{\nu_l'^2}\left[\,A^l_{2S}\{(-iq_l')(iq_l)+p^2\cos\theta\}+A^l_{2T}(ik_2)(ip)\sin\theta\,\right]\\
\bar{A}^l_{2T} &= \frac{1}{\nu_l'^2}\left[\,A^l_{2S}(ik_2)(ip)\sin\theta+A^l_{2T}\{(-iq_l')(iq_l)+p^2\cos\theta\}\,\right]
\end{aligned}
\right\} \quad (4.3.10)
$$

$$
\left.
\begin{aligned}
\bar{B}^l_{2S} &= -\frac{r_l'^2+\sqrt{\nu_l'^2+k_3^2}}{\sqrt{\nu_l'^2+k_2^2}+\sqrt{\nu_l'^2+k_3^2}}\,e^{-\sqrt{\nu_l^2+k_2^2}D}\,\bar{A}^l_{2S}\\
\bar{A}^l_{3S} &= -\frac{k_3}{k_2}\frac{r_l'^2-\sqrt{\nu_l'^2+k_2^2}}{\sqrt{\nu_l'^2+k_2^2}+\sqrt{\nu_l'^2+k_3^2}}\,e^{-\sqrt{\nu_l^2+k_2^2}D}\,\bar{A}^l_{2S}\\
\bar{B}^l_{2T} &= -\frac{r_l'^2+\frac{k_2^2}{k_3^2}\sqrt{\nu_l'^2+k_3^2}}{\sqrt{\nu_l'^2+k_2^2}+\frac{k_2^2}{k_3^2}\sqrt{\nu_l'^2+k_3^2}}\,e^{-\sqrt{\nu_l^2+k_2^2}D}\,\bar{A}^l_{2T}\\
\bar{A}^l_{3T} &= -\frac{r_l'^2-\sqrt{\nu_l'^2+k_2^2}}{\sqrt{\nu_l'^2+k_2^2}+\frac{k_2^2}{k_3^2}\sqrt{\nu_l'^2+k_3^2}}\,e^{-\sqrt{\nu_l^2+k_2^2}D}\,\bar{A}^l_{2T}
\end{aligned}
\right\} \quad (4.3.11)
$$

$$
\left.
\begin{aligned}
B^l_{2S} &= \frac{1}{\nu_{l+1}^2}\left[\,\bar{B}^l_{2S}\{(-iq_l')(iq_{l+1})+p^2\cos\theta\}+\bar{B}^l_{2T}(ik_2)(-ip)\sin\theta\,\right]\\
B^l_{2T} &= \frac{1}{\nu_{l+1}^2}\left[\,\bar{B}^l_{2S}(ik_2)(-ip)\sin\theta+\bar{B}^l_{2T}\{(-iq_l')(iq_{l+1})+p^2\cos\theta\}\,\right]
\end{aligned}
\right\} \quad (4.3.12)
$$

$$
\left.
\begin{aligned}
B_{1S}^{l+1} &= \frac{k_1}{k_2}\,\frac{\Gamma_{l+1}+\sqrt{\nu_{l+1}^2+k_2^2}}{\sqrt{\nu_{l+1}^2+k_1^2}+\sqrt{\nu_{l+1}^2+k_2^2}}\,e^{-\Gamma_{l+1}D}\,B_{2S}^{l}\\
A_{2S}^{l+1} &= \frac{\Gamma_{l+1}-\sqrt{\nu_{l+1}^2+k_2^2}}{\sqrt{\nu_{l+1}^2+k_1^2}+\sqrt{\nu_{l+1}^2+k_2^2}}\,e^{-\Gamma_{l+1}D}\,B_{2S}^{l}\\
B_{1T}^{l+1} &= \frac{\Gamma_{l+1}+\sqrt{\nu_{l+1}^2+k_2^2}}{\sqrt{\nu_{l+1}^2+k_2^2}+\frac{k_2^2}{k_1^2}\sqrt{\nu_{l+1}^2+k_1^2}}\,e^{-\Gamma_{l+1}D}\,B_{2T}^{l}\\
A_{2T}^{l+1} &= \frac{\Gamma_{l+1}-\frac{k_2^2}{k_1^2}\sqrt{\nu_{l+1}^2+k_1^2}}{\sqrt{\nu_{l+1}^2+k_2^2}+\frac{k_2^2}{k_1^2}\sqrt{\nu_{l+1}^2+k_1^2}}\,e^{-\Gamma_{l+1}D}\,B_{2T}^{l}
\end{aligned}
\right\} \quad (4.3.13)
$$

4–4. The second type field as an external field

Following a successive procedure similar to that in the previous sub-section, we can solve the problem when the second type field is incident to such an underground structure as shown in Figure 3. Even in this case, the solutions obtained in the previous section hold true except for the equations (4.3.1) and (4.3.2), which should be replaced by the following,

$$
\left.
\begin{aligned}
B_{1T}^{0} &= \frac{\sqrt{\nu^2+k_1^2}+\frac{k_1^2}{k_2^2}\sqrt{\nu^2+k_2^2}}{\sqrt{\nu^2+k_1^2}+\frac{k_1^2}{k_2^2}\sqrt{\nu^2+k_2^2}}\,A_{1T}^{0}\\
A_{2T}^{0} &= \frac{2\sqrt{\nu^2+k_1^2}}{\sqrt{\nu^2+k_1^2}+\frac{k_1^2}{k_2^2}\sqrt{\nu^2+k_2^2}}\,A_{1T}^{0}
\end{aligned}
\right\} \quad (4.4.1)
$$

$$
\left.
\begin{aligned}
\bar{A}_{2S}^{0} &= \frac{1}{\nu'^2}\left[\, ik_2(ip)\sin\theta \,\right] A_{2T}^{0}\\
\bar{A}_{2T}^{0} &= \frac{1}{\nu'^2}\left[\, -iq)(iq') + p^2\cos\theta \,\right] A_{2T}^{0}
\end{aligned}
\right\} \quad (4.4.2)
$$

4–5. Both types of fields as external fields

Repetition of the above procedure enables us to solve the problem when both the first and the second type fields are considered together as the external applied field. Almost all the solutions take exactly the same forms as are listed in the section 4–3. The only difference is that the first two solutions (4.3.1) and (4.3.2) should be replaced by the following.

$$
\left.
\begin{aligned}
A_{2S}^{0} &= \frac{k_2}{k_1}\,\frac{2\sqrt{\nu^2+k_1^2}}{\sqrt{\nu^2+k_1^2}+\sqrt{\nu^2+k_2^2}}\,A_{1S}^{0}\\
B_{1S}^{0} &= \frac{\sqrt{\nu^2+k_1^2}-\sqrt{\nu^2+k_2^2}}{\sqrt{\nu^2+k_1^2}+\sqrt{\nu^2+k_2^2}}\,A_{1S}^{0}
\end{aligned}
\right\} \quad (4.3.1)
$$

$$B^0_{1T} = \frac{\sqrt{\nu^2+k_1^2} - \frac{k_1^2}{k_2^2}\sqrt{\nu^2+k_2^2}}{\sqrt{\nu^2+k_1^2} + \frac{k_1^2}{k_2^2}\sqrt{\nu^2+k_2^2}} A^0_{1T}$$

$$A^0_{2T} = \frac{2\sqrt{\nu^2+k_1^2}}{\sqrt{\nu^2+k_1^2} + \frac{k_1^2}{k_2^2}\sqrt{\nu^2+k_2^2}} A^0_{1T} \qquad (4.5.1)$$

$$\bar{A}^0_{2S} = \frac{1}{\nu'^2}[A^0_{2S}\{(-iq)(iq') + p^2\cos\theta\} + A^0_{2T}(ik_2)(ip)\sin\theta]$$

$$\bar{A}^0_{2T} = \frac{1}{\nu'^2}[A^0_{2S}(ik_2)(ip)\sin\theta + A^0_{2T}\{(-iq)(iq') + p^2\cos\theta\}] \qquad (4.5.2)$$

4–6. Electromagnetic field at the surface of the ground

The magnetic field and the electric field in the region (I) can be approximated by an infinite series as follows,

$$\mathbf{H} = A^0_{1S}{}^0\mathbf{H}^{1e}_S + B^0_{1S}{}^0\mathbf{H}^{1i}_S + B^1_{1S}{}^1\mathbf{H}^{1i}_S + B^1_{1T}{}^1\mathbf{H}^{1i}_T + \cdots$$

$$\mathbf{E} = A^0_{1S}{}^0\mathbf{E}^{1e}_T + B^0_{1S}{}^0\mathbf{E}^{1i}_T + B^1_{1S}{}^1\mathbf{E}^{1i}_T + B^1_{1T}{}^1\mathbf{E}^{1i}_S + \cdots \qquad (4.6.1)$$

Substituting the equation (4.2.1) into the above, we have

$$\mathbf{H} = \frac{A^0_{1S}}{ik_1}\begin{bmatrix} -ip\sqrt{\nu^2+k_1^2} \\ -iq\sqrt{\nu^2+k_1^2} \\ \nu^2 \end{bmatrix}\psi^0_{1e} + \frac{B^0_{1S}}{ik_1}\begin{bmatrix} ip\sqrt{\nu^2+k_1^2} \\ iq\sqrt{\nu^2+k_1^2} \\ \nu^2 \end{bmatrix}\psi^0_{1i} + \frac{B^1_{1S}}{ik_1}\begin{bmatrix} ip\sqrt{\nu_1^2+k_1^2} \\ iq_1\sqrt{\nu_1^2+k_1^2} \\ \nu_1^2 \end{bmatrix}\psi^1_{1i} + B^1_{1T}\begin{bmatrix} iq_1 \\ -ip \\ 0 \end{bmatrix}\psi^1_{1i} + \cdots$$

$$\mathbf{E} = -\frac{A^0_{1S}}{k_1}\omega\mu\begin{bmatrix} iq \\ -ip \\ 0 \end{bmatrix}\psi^0_{1e} - \frac{B^0_{1S}}{k_1}\omega\mu\begin{bmatrix} iq \\ -ip \\ 0 \end{bmatrix}\psi^0_{1i} - \frac{B^1_{1S}}{k_1}\omega\mu\begin{bmatrix} iq_1 \\ -ip \\ 0 \end{bmatrix}\psi^1_{1i} + \frac{B^1_{1T}}{k_1^2}i\omega\mu\begin{bmatrix} ip\sqrt{\nu_1^2+k_1^2} \\ iq_1\sqrt{\nu_1^2+k_1^2} \\ \nu_1^2 \end{bmatrix}\psi^1_{1i} + \cdots$$

Since the coefficients B^0_{1S}, B^1_{1S}, ..., B^1_{1T}, B^2_{1T} ... are calculated in the section 4–3 and $\psi^l_{1(e,i)}$ at $z = 0$ is easily obtained from the equation (4.2.2), we can calculate the magnetic field and the electric field at the ground surface from the above equations. However, the coefficients $B^l_{1(S,T)}$ are expressed in such complicated forms that it is not an easy matter to see the general behaviour of the electromagnetic field without making numerical calculations. The results of numerical calculations using an electronic computer are shown in a later section. In this section, only a few special cases, which are tractable in an approximate way, are discussed.

Case: $k_1^2 = k_2^2$; $\nu^2 \gg k_1^2, k_2^2$; $k_3^2 \gg k_2^2, k_1^2$

This is a case in which the second layer (II) is identical with the poorly conducting first layer (I). Then all the energy of the electromagnetic field, whether it be the field incident from outside the earth or the field reflected from

the tilted boundary, will be transmitted perfectly through the interface (I–II). Consequently, on employing the successive approximation presented in a previous section, we have only to consider the first reflection at the tilted boundary (II–III).

Ignoring k_1^2, k_2^2, compared with ν^2, the coefficients of (4.3.1) to (4.3.5) are simplified as follows,

$$\left.\begin{aligned} B_{1S}^0 &= 0 \\ A_{2S}^0 &= A_{1S}^0 \end{aligned}\right\} \quad (4.6.3)$$

$$\left.\begin{aligned} \bar{A}_{2S}^0 &= \frac{1}{\nu'^2}(q\cdot q' + p^2\cos\theta)\bar{A}_{2S}^0 \\ \bar{A}_{2T}^0 &= -\frac{1}{\nu'^2}k_2 p \sin\theta\ \bar{A}_{2S}^0 \end{aligned}\right\} \quad (4.6.4)$$

$$\left.\begin{aligned} \bar{B}_{2S}^0 &= \phi(\nu', k_3)e^{-\sqrt{\nu^2+k_2^2}D}\bar{A}_{2S}^0 \ , \quad \phi(\nu', k_3) = \frac{\nu' - \sqrt{\nu'^2+k_3^2}}{\nu' + \sqrt{\nu'^2+k_3^2}} \\ \bar{B}_{2T}^0 &= e^{-\sqrt{\nu^2+k_2^2}D}\bar{A}_{2T}^0 \end{aligned}\right\} \quad (4.6.5)$$

$$\left.\begin{aligned} B_{2S}^0 &= \frac{1}{\nu_1}[(q'\cdot q_1 + p^2\cos\theta)\bar{B}_{2S}^0 + ik_2(-ip)\sin\theta\,\bar{B}_{2T}^0] \\ B_{2T}^0 &= \frac{1}{\nu_1}[ik_2(-ip)\sin\theta\bar{B}_{2S}^0 + (q'\cdot q_1 + p^2\cos\theta)\bar{B}_{2T}^0] \end{aligned}\right\} \quad (4.6.6)$$

$$\left.\begin{aligned} A_{2S}^1 &= 0 \\ A_{2T}^1 &= 0 \end{aligned}\right\} \quad (4.6.7)$$

$$\left.\begin{aligned} B_{1S}^1 &= e^{-r_1 D}B_{2S}^0 \\ B_{1T}^1 &= e^{-r_1 D}B_{2T}^0 \end{aligned}\right\} \quad (4.6.8)$$

Since $\nu^2 \gg k_2^2, k_1^2$, we have the following relationships between the wave numbers,

$$\left.\begin{aligned} \nu' &= \nu\cos\theta + iq\sin\theta \\ \nu_1 &= \nu\cos 2\theta + iq\sin 2\theta \\ q' &= q\cos\theta + i\nu\sin\theta \\ q_1 &= q\cos 2\theta + i\nu\sin 2\theta \end{aligned}\right\} \quad (4.6.9)$$

Therefore the equations (4.6.4) to (4.6.8) can be rewritten as follows,

$$
\left.
\begin{aligned}
\overline{A}^0_{2S} &= \frac{\nu}{\nu'} A^0_{1S} \\
\overline{A}^0_{2T} &= -\frac{k_2 p \sin\theta}{\nu'^2} A^0_{1S} \\
\overline{B}^0_{2S} &= \phi(\nu', k_3)\, e^{-\sqrt{\nu^2+k_2^2}D} \frac{\nu}{\nu'} A^0_{1S} \\
\overline{B}^0_{2T} &= -\frac{k_2 p \sin\theta}{\nu'^2} e^{-\sqrt{\nu^2+k_2^2}D} A^0_{1S} \\
B^0_{2S} &= \phi(\nu', k_3)\, e^{-\sqrt{\nu^2+k_2^2}D} \frac{\nu}{\nu_1} A^0_{1S} \\
B^0_{2T} &= -\frac{k_2 p \sin\theta}{\nu' \cdot \nu_1} e^{-\sqrt{\nu^2+k_2^2}D} \left[-\frac{\nu}{\nu_1}\phi(\nu', k_3) + 1\right] A^0_{1S} \\
B^1_{1S} &= \phi(\nu', k_3)\, e^{-\{r_1+\sqrt{\nu^2+k_2^2}\}D} \frac{\nu}{\nu_1} A^0_{1S} \\
B^1_{1T} &= -\frac{k_2 p \sin\theta}{\nu' \cdot \nu_1} e^{-\{r_1+\sqrt{\nu^2+k_2^2}\}D} \left[-\frac{\nu}{\nu_1}\phi(\nu', k_3) + 1\right] A^0_{1S}
\end{aligned}
\right\} \quad (4.6.10)
$$

Substituting these in the equation (4.6.2) and putting $z = 0$, $y = 0$, we have the following equations for the electromagnetic field at the ground surface (I–II).

$$
\left.
\begin{aligned}
H_x &= -\frac{p\nu}{k_1}\left[1-\phi(\nu', k_3)\, e^{-(\nu_1+\nu)D}\right] A^0_{1S} \\
H_y &= -\frac{q\nu}{k_1}\left[1-\frac{q_1}{q}\phi(\nu', k_3)\, e^{-(\nu_1+\nu)D}\right] A^0_{1S} \\
H_z &= \frac{\nu^2}{ik_1}\left[1+\frac{\nu_1}{\nu}\phi(\nu', k_3)\, e^{-(\nu_1+\nu)D}\right] A^0_{1S} \\
E_x &= -\frac{\omega\mu}{k_1}(iq)\left[1+\frac{q_1}{q}\frac{\nu}{\nu_1}\phi(\nu', k_3)\, e^{-(\nu_1+\nu)D} + i\frac{p^2 \sin\theta}{q\cdot\nu'} e^{-(\nu_1+\nu)D}\{1-\frac{\nu}{\nu_1}\phi(\nu', k_3)\}\right] A^0_{1S} \\
E_y &= \frac{\omega\mu}{k_1}(ip)\left[1+\frac{\nu}{\nu_1}\phi(\nu', k_3)\, e^{-(\nu_1+\nu)D} - i\frac{q_1 \sin\theta}{\nu'} e^{-(\nu_1+\nu)D}\{1-\frac{\nu}{\nu_1}\phi(\nu', k_3)\}\right] A^0_{1S}
\end{aligned}
\right\} \quad (4.6.11)
$$

When σ_3 is large ($k_3^2 \gg \nu'^2$), we have approximately $\phi(\nu', k_3) = -1$. Provided that θ is small, trigonometric functions can be approximated by power series of θ. Then, ignoring terms higher than θ^6, we can rewrite the above equations as follows,

$$
H_x = -\frac{p\nu}{k_1}\left[1 + e^{-(\nu_1+\nu)D}\right] A^0_{1S}
$$

$$H_y = -\frac{q\nu}{k_1}\left[1+\{1-2\theta^2+i\,2\frac{\nu}{q}\theta(1-\tfrac{1}{3}\theta^2)\}e^{-(\nu_1+\nu)D}\right] A^0_{1S}$$

$$H_z = \frac{\nu^2}{ik_1}\left[1-e^{-(\nu_1+\nu)D}+2\,\theta^2\{1-\tfrac{1}{3}\theta^2\}e^{-(\nu_1+\nu)D}-i\,\frac{q}{\nu}\,2\theta\{1-\tfrac{2}{3}\theta^2+\tfrac{2}{15}\theta^4\}e^{-(\nu_1+\nu)D}\right] A^0_{1S}$$

$$E_x = -\frac{\omega\mu}{k_1}\,iq\left[1-e^{-(\nu_1+\nu)D}\right] A^0_{1S}$$

$$E_y = \frac{\omega\mu}{k_1}\,(ip)\left[1-e^{-(\nu_1+\nu)D}+2\,\theta^2 e^{-(\nu_1+\nu)D}\right] A^0_{1S}$$

When $\nu D \gg 1$, and neglecting terms of the order of θ^3 and $\nu D\cdot\theta^2$, we have

$$H_x = -\frac{2p\nu}{k_1}\left[1-\nu D-iq\,\theta\,D\right] A^0_{1S}$$

$$H_y = -\frac{2q\nu}{k_1}\left[1-\nu D+i\frac{\nu}{q}\,\theta(1-\frac{q^2D}{\nu})\right] A^0_{1S}$$

$$H_z = -\frac{2\nu^2}{k_1}\left[\frac{q}{\nu}\,\theta(1-\nu D)+i(\nu D+\theta^2)\right] A^0_{1S}$$

$$E_x = -\frac{2\omega\mu}{k_1}\,(iq)\left[\nu D+iq\theta D\right] A^0_{1S}$$

$$E_y = \frac{2\omega\mu}{k_1}\,(ip)\left[\nu D+\theta^2+iq\theta D\right] A^0_{1S}$$

When $\nu D \gg \theta^2 \gg 1$, the above equations become

$$\left.\begin{aligned}
H_x &= -\frac{2p\nu}{k_1}\,A^0_{1S}\\
H_y &= -\frac{2q\nu}{k_1}\left[1+i\frac{\nu}{q}\theta\right] A^0_{1S}\\
H_z &= -\frac{2q\nu}{k_1}\,\theta\left[1+i\frac{\nu}{q}\theta\right] A^0_{1S}\\
E_x &= -\frac{2\omega\mu}{k_1}\,(iq)\,\nu D\left[1+i\frac{q}{\nu}\theta\right] A^0_{1S}\\
E_y &= \frac{2\omega\mu}{k_1}\,(ip)\,\theta^2\left[1+i\,\frac{qD}{\theta}\right] A^0_{1S}\\
\frac{E_x}{H_y} &= i\omega\mu D\,\frac{1+i\frac{q}{\nu}\theta}{1+i\frac{\nu}{q}\theta}\\
\frac{E_y}{H_x} &= -\,i\omega\mu\theta^2\,\frac{p}{\nu q}\cdot\frac{1+i\frac{qD}{\theta}}{1+i\frac{\nu}{q}\theta}
\end{aligned}\right\} \quad (4.6.12)$$

From these, we may conclude that (i) the horizontal components of the magnetic field (H_x, H_y) are made twice as large as the applied external field by the existence of a highly conducting layer dipping with a small angle; (ii) the ratio of H_z to H_y always remains constant ($H_z/H_y=\theta$) irrespective of H_x, or of the orientation of the horizontal vector of the magnetic field; this indicates that the magnetic variation vectors are confined on a plane parallel to the tilted boundary; (iii) the ratio of E_y to E_x is of the order of $\theta^2/\nu D$; consequently the variation of the electric field at the ground surface is expected to be polarized linearly in the y–direction; (iv) E_x/H_y is equivalent to that of the horizontal case (3.21) except for a correction factor $\dfrac{1+i\frac{q}{\nu}\theta}{1+i\frac{\nu}{q}\theta}$, whereas E_y/H_x is essentially different from (3.21) due to the effect of the dipping boundary.

On the other hand, when $1 \gg \nu D \gg \theta$, we have the following equations in place of (4.6.12).

$$\left.\begin{aligned} H_x &= -\frac{2p\nu}{k_1}[1-\nu D]\,A_{1S}^0 \\ H_y &= -\frac{2q\nu}{k_1}[1-\nu D]\,A_{1S}^0 \\ H_z &= -i\frac{2\nu^2}{k_1}\nu D\,A_{1S}^0 \\ E_x &= -\frac{2\omega\mu}{k_1}(iq)\cdot\nu D \\ E_y &= \frac{2\omega\mu}{k_1}(ip)\cdot\nu D \end{aligned}\right\} \quad (4.6.13)$$

Therefore if we take the ratio of H_z to either H_x or H_y, we have

$$\left.\frac{H_z}{\{H_x, H_y\}} = \frac{i\nu}{\{p, q\}}\cdot\frac{\nu D}{1-\nu D}\right\} \quad (4.6.14)$$

This is equivalent to the equation (3.22) obtained in the case of horizontally stratified structure. In a similar way we have

$$\left.\begin{aligned} \frac{E_x}{H_y} &= \frac{i\omega\mu D}{1-\nu D} \\ \frac{E_y}{H_x} &= -\frac{i\omega\mu D}{1-\nu D} \end{aligned}\right\} \quad (4.6.15)$$

This is also the same as the equation (3.21), and no preferred direction of the telluric field variation is obtained in this case.

5. Numerical Calculation

5–1. Process of numerical calculation

Since it is not possible to obtain analytically simple expressions for many cases of interest, the problem was solved numerically on a CDC 3400 electronic computer, at the University of Montreal, for a few specific earth models in which the first type field is applied from outside the earth.

The program was arranged so as to follow the iterative process decribed in section 4. In the first place, B^0_{1S}, A^0_{2S} and then $\bar{A}^0_{2S}$, $\bar{A}^0_{2T}$ were computed from the equations (4.3.1), (4.3.2). The complex coefficients $\bar{A}^0_{2S}$ $\bar{A}^0_{2T}$ were used to calculate $\bar{B}^0_{2S}$, $\bar{B}^0_{2T}$, $\bar{A}^0_{3S}$ and $\bar{A}^0_{3T}$ following the process shown in the equations (4.3.3). Then $\bar{B}^0_{2S}$ and $\bar{B}^0_{2T}$ were transformed into B^0_{2S} and B^0_{2T} by (4.3.4). From these, B^1_{1S}, B^1_{1T} and A^1_{2S}, A^1_{2T} in (4.3.5) were obtained in complex forms. Substituting A^1_{2S}, A^1_{2T} into (4.3.6), we could compute $\bar{A}^1_{2S}$, $\bar{A}^1_{2T}$. Then repeating the same procedure, B^2_{1S}, B^2_{1T}, . . . , B^l_{1S}, B^l_{1T} were computed.

On the other hand, the magnetic field and the electric field at $y = 0$, $z = 0$ are expressed, in the case when $k_1 \ll 1$, as follows,

$$H_x = \frac{p\nu}{k_1} A^0_{1S}\left[-1 + \sum_{l=0}^{\infty} \Delta H^l_x\right]$$

$$H_y = \frac{p\nu}{k_1} A^0_{1S}\left[-1 + \sum_{l=0}^{\infty} \Delta H^l_y\right]$$

$$H_z = -\frac{i\nu^2}{k_1} A^0_{1S}\left[1 + \sum_{l=0}^{\infty} \Delta H^l_z\right]$$

$$E_x = \frac{i\omega\mu q}{k_1} A^0_{1S}\left[1 + \frac{B^0_{1S}}{A^0_{1S}} + \sum_{l=0}^{\infty} \Delta E^l_x\right]$$

$$E_y = -\frac{i\omega\mu p}{k_1} A^0_{1S}\left[1 + \frac{B^0_{1S}}{A^0_{1S}} + \sum_{l=0}^{\infty} \Delta E^l_y\right]$$

where $\Delta H^l_x = \dfrac{\nu_l}{\nu}\dfrac{B^l_{1S}}{A^0_{1S}}$

$$\Delta H^l_y = \frac{\nu_l}{\nu}\frac{q_l}{q}\frac{B^l_{1S}}{A^0_{1S}}$$

$$\Delta H^l_z = \frac{\nu_l^2}{\nu^2}\frac{B^l_{1S}}{A^0_{1S}}$$

$$\Delta E^l_x = \frac{q_l}{q}\frac{B^l_{1S}}{A^0_{1S}} + \frac{p}{q}\nu_l\frac{B^l_{1T}}{A^0_{1S}}$$

$$\Delta E^l_y = \frac{B^l_{1S}}{A^0_{1S}} - \frac{q_l}{p}\nu_l\frac{B^l_{1T}}{A^0_{1S}}$$

Every time B_{1S} and B_{1T} were obtained, $\Delta H^l_{x,y,z}$ and $\Delta E^l_{x,y}$ were computed. The above procedure of obtaining B^l_{1S} and B^l_{1T} was repeated until the terms $\Delta H^l_{x,y,z}$ and $\Delta E^l_{x,y}$ became less than 10^{-3}.

The program for the tilted boundary was shown to be working properly by making computer calculations for a few special cases, where the solutions were obtainable analytically, such as the case when $\theta = 0^\circ$ or the case discussed in the following section.

5–2. Results of numerical calculation

Table I gives values of the essential parameters for three models – A, B and C. The amplitude and phase relationships of the magnetic and electric ratios and their dependence on source field wave length, angles of tilt and period, are discussed in this section.

Table I

	σ_2 emu	σ_3 emu	θ^0	D km	k_1^2/k_2^2
Model A	10^{-30}	10^{-11}	10	10	1
Model B	10^{-15}	10^{-11}	10	10	10^{-39}
Model C	10^{-11}	10^{-15}	10	10	10^{-39}

a) Anisotropic behaviour of the electric field.

a–i) Model A with $\nu = 10^{-10}$ cm^{-1}

This model is a tilted conductor underlying a highly resistive layer. Hodograms of the magnetic and electric horizontal vectors for variable p or q ($\nu^2 = p^2 + q^2$) and T = 100 sec are given in Figure 8. It is seen that the electric vector is strongly polarized for the majority of the magnetic source orientations.

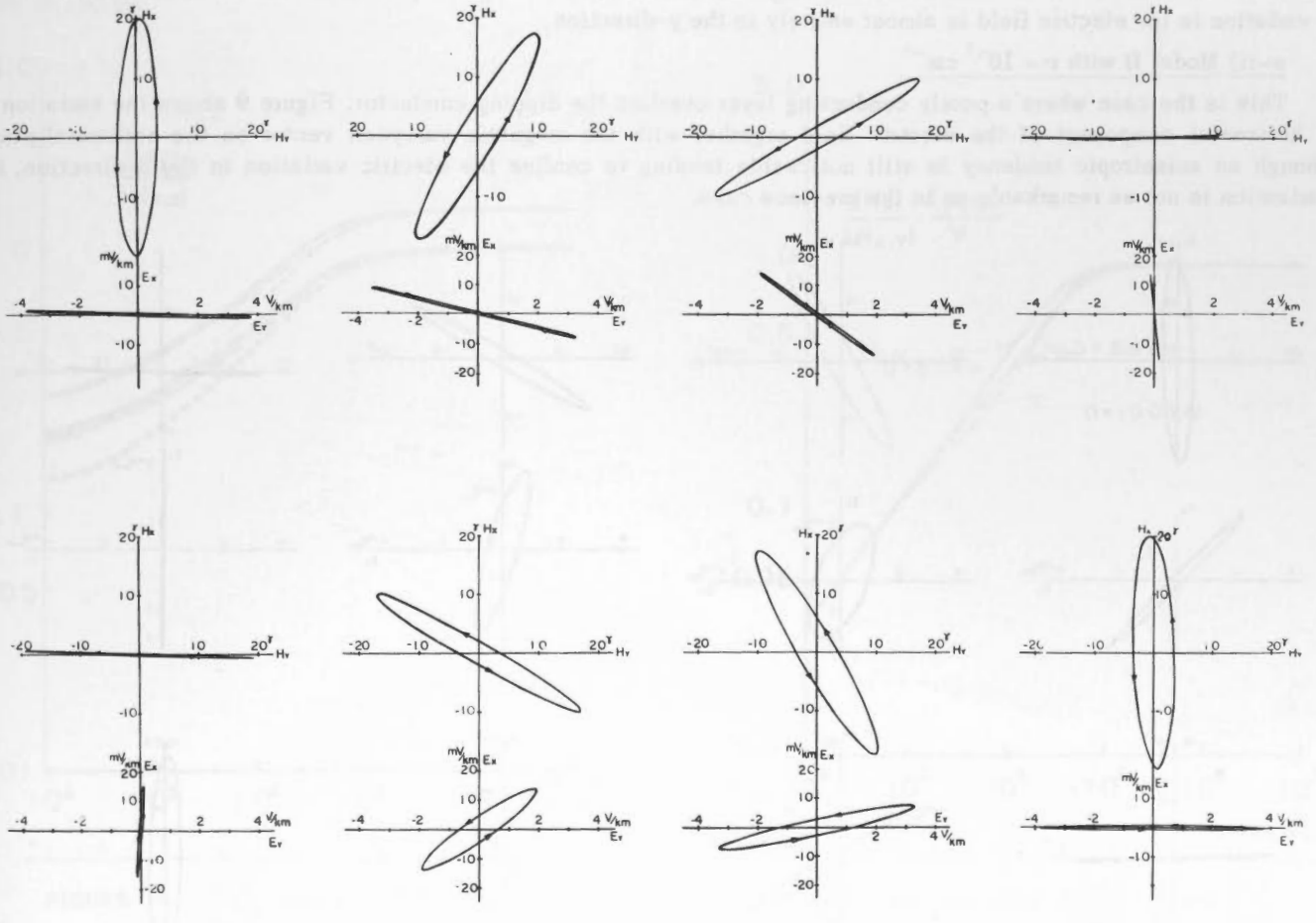

FIGURE 8. Variations in the horizontal components of the magnetic and the electric field in the case where $\nu = 10^{-10}$cm^{-1}, T = 100 sec, $k_1^2/k_2^2 = 1$, $\sigma_2 = 10^{-30}$emu, $\sigma_3 = 10^{-11}$emu, $\theta = 10^0$, D = 10 km.

The ratios H_z/H_x, H_z/H_y, E_y/E_x are given in Table II for p = q = 0.7071 x 10^{-10} cm^{-1} and for the periods 10^2, 10^4, and 10^5 sec. The electric ratio is always large throughout this period range indicating strong polarization in the y–direction, although this effect decreases somewhat (one order of magnitude) with increasing period. In contrast, for the same source orientation the ratios H_z/H_y, H_z/H_x remain nearly constant in this period range and are equivalent to the angle of tilt of the plane. However, on changing the orientation (ie p or q) of the magnetic source vector, the

ratio H_z/H_y, varies in amplitude and in phase (not illustrated), while H_z/H_y remains constant ($H_z/H_y = .176 = \tan 10^0$).

Table II

H_z/H_x, H_z/H_y, and E_y/E_x for $\theta = 10^0$, $\nu = 10^{-10}\text{cm}^{-1}$, p = q, $\sigma_2 = 10^{-30}$emu, $\sigma_3 = 10^{-11}$emu, $k_1^2 = k_2^2$.

	T = 10^2 sec		T = 10^4 sec		T = 10^5 sec	
	Ampl.	Phase	Ampl.	Phase	Ampl.	Phase
H_z/H_x	0.176	0.0781π	0.177	0.0787π	0.177	0.0800π
H_z/H_y	0.176	0.0003π	0.177	0.0009π	0.178	0.0023π
E_y/E_x	236.3	-0.984π	69.0	-0.874π	25.5	-0.852π

The above results can be deduced from equations (4.6.12) for the particular combination of parameters $\nu D \ll \theta^2 \ll 1$. It is concluded that, for this case, the magnetic field varies on a plane parallel to the tilted boundary and that the variation in the electric field is almost entirely in the y–direction.

a–ii) Model B with $\nu = 10^{-7}$ cm^{-1}

This is the case where a poorly conducting layer overlies the dipping conductor. Figure 9 shows the variation in the horizontal component of the electric field together with the magnetic variation vector on the horizontal plane. Although an anisotropic tendency is still noticeable tending to confine the electric variation in the x–direction, the polarization is not as remarkable as in the previous case.

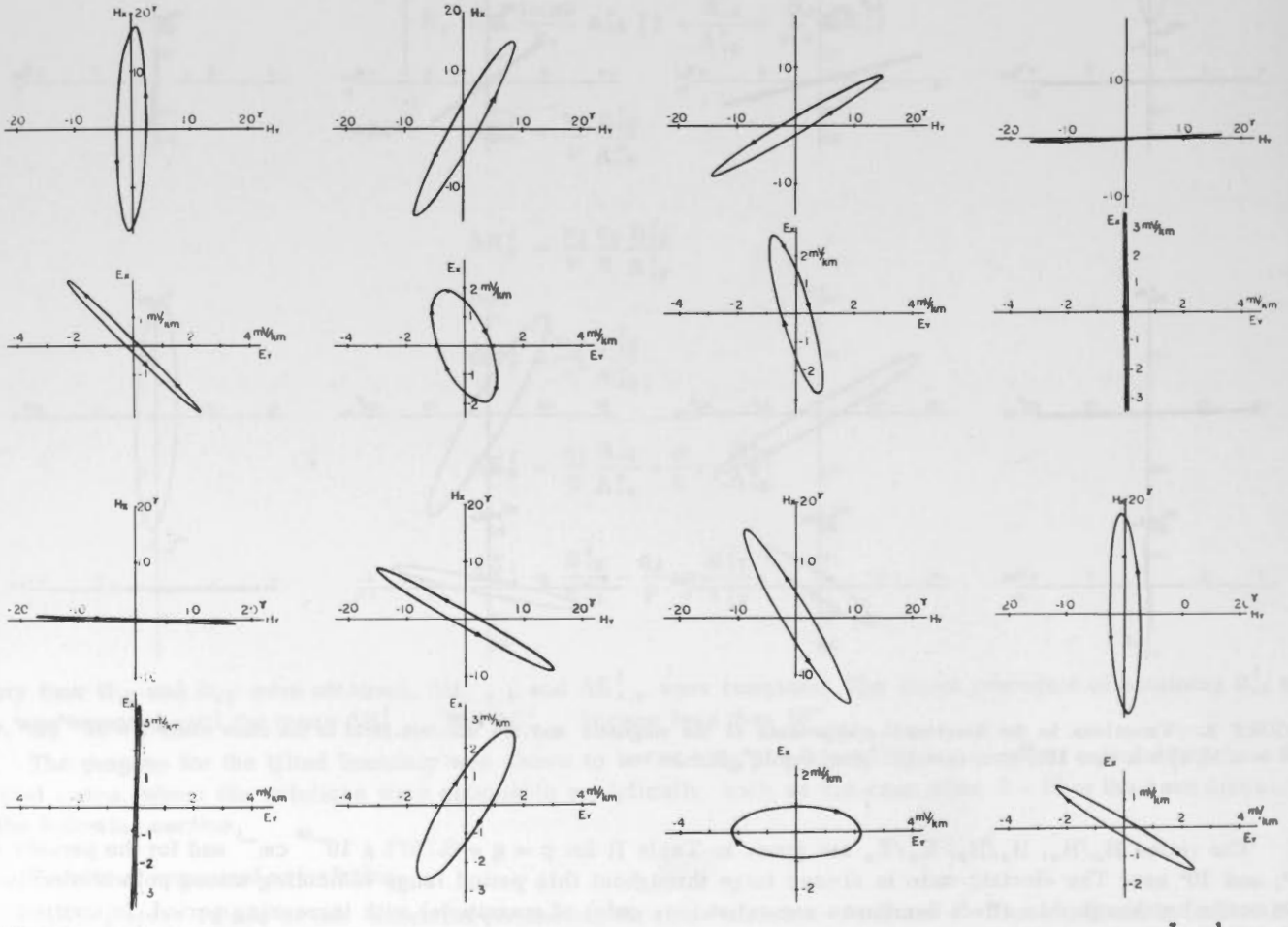

FIGURE 9. Variations in the horizontal components of the magnetic and the electric field in the case where $\nu = 10^{-7}\text{cm}^{-1}$, T = 500 sec, $k_1^2/k_2^2 = 10^{-39}$, $\sigma_2 = 10^{-15}$emu, $\sigma_3 = 10^{-11}$emu, $\theta = 10^0$, D = 10 km.

When the magnetic vector rotates as in Figure 9, H_z/H_y varies from 0.17 to 1.3. It follows that the magnetic variation is not confined to a plane in this case.

Consequently it is clear that the existence of a poor conductor over the dipping conductor leads to differences in the magnetic and electric variations when compared with the case in which the atmosphere is in direct contact with the tilted conductor.

b) Magnetic component ratios

$\frac{H_z}{H_x} \cdot \frac{p}{\nu}$ and $\frac{H_z}{H_y} \cdot \frac{q}{\nu}$ were calculated for Model B with $\nu = 10^{-7}$ cm^{-1}, p = q = 0.7071 x 10^{-7} cm^{-1}, and are shown in Figure 10 together with similar curves for the horizontal structure. Slight differences between the curves for $\frac{H_z}{H_x} \cdot \frac{p}{\nu}$ can be seen for shorter periods only.

In Figure 11, the ratios are shown for model C in which the good conductor overlies a poorly conducting tilted material. The parameters chosen were $\theta = 10^0$, $\sigma_2 = 10^{-11}$emu, $\sigma_3 = 10^{-15}$emu, $\nu = 10^{-7}$ cm^{-1}, p = q, $\frac{k_1^2}{k_2^2} = 10^{-39}$. The figure indicates that the magnetic variation loses its anisotropic property when the dipping boundary is placed at a depth of 100 km.

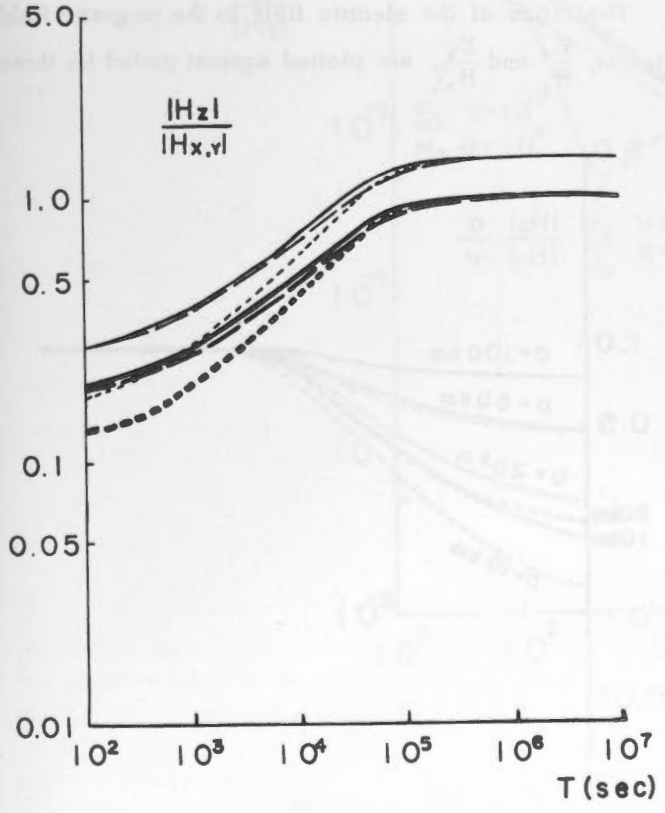

FIGURE 10. $\frac{|H_z|}{|H_{x,y}|}$ when $\nu = 10^{-7}$cm^{-1}, p = q, $\sigma_2 = 10^{-15}$emu, $\sigma_3 = 10^{-11}$emu, $k_1^2/k_2^2 = 10^{-39}$, $\theta = 10^0$, D = 10 km. Thin solid line represents $\frac{H_z}{H_y}$: heavy solid line, $\frac{H_z}{H_y} \cdot \frac{q}{\nu}$: thin broken line, $\frac{H_z}{H_x} \cdot \frac{p}{\nu}$. Thin dotted line represents $\frac{H_z}{H_{x,y}}$ for $\theta = 0^0$: heavy dotted line, $\frac{H_z}{H_{x,y}} \cdot \frac{(p,q)}{\nu}$ for $\theta = 0^0$.

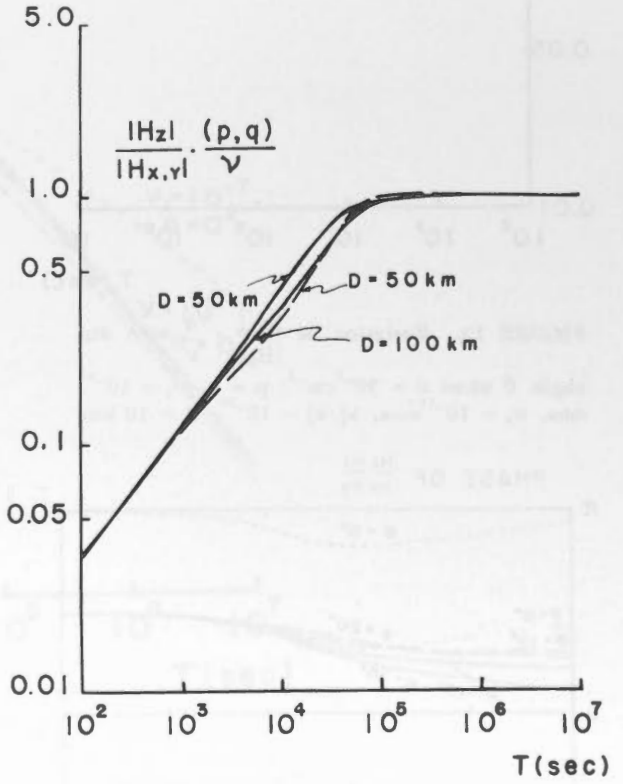

FIGURE 11. Variation of $\frac{|H_z|}{|H_x|} \cdot \frac{p}{\nu}$ and $\frac{|H_z|}{|H_y|} \cdot \frac{q}{\nu}$ with depth when $\nu = 10^{-7}$cm^{-1}, p = q, $\sigma_2 = 10^{-11}$emu, $\sigma_3 = 10^{-15}$emu, $k_1^2/k_2^2 = 10^{-39}$, $\theta = 10^0$. Solid lines represent $\frac{H_z}{H_y} \frac{q}{\nu}$, broken lines $\frac{H_z}{H_x} \frac{p}{\nu}$. No difference between $\frac{H_z}{H_x} \frac{p}{\nu}$ and $\frac{H_z}{H_y} \frac{q}{\nu}$ can be seen in the case of D = 100 km.

When the angle of tilt θ is changed from 0° to 20° the ratio $\frac{H_z}{H_y} \cdot \frac{q}{\nu}$ changes as is shown in Figure 12. It is evident that tilting the boundary causes the ratio to increase above its value for the horizontally stratified model. Phase differences of $\frac{H_z}{H_y}$, $\frac{H_z}{H_x}$ are given in Figure 13.

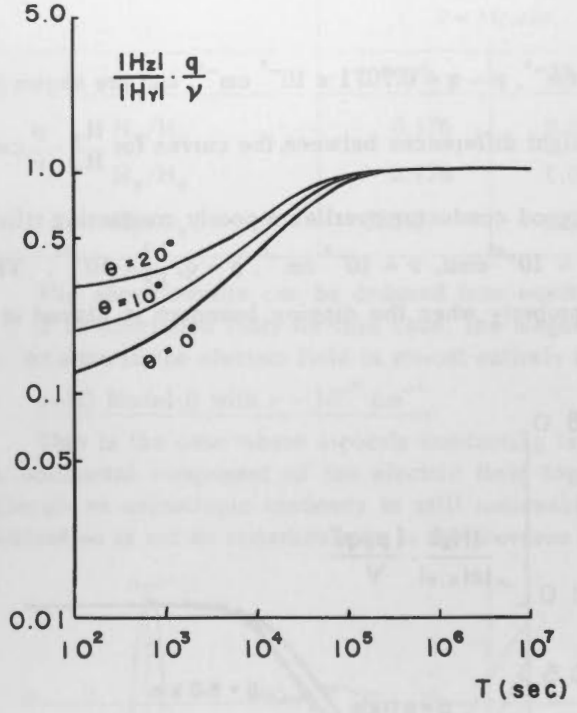

FIGURE 12. Variation of $\frac{|H_z|}{|H_y|} \cdot \frac{q}{\nu}$ with dip angle θ when $\nu = 10^{-7}\text{cm}^{-1}$; p = q, $\sigma_2 = 10^{-15}$ emu, $\sigma_3 = 10^{-11}$ emu, $k_1^2/k_2^2 = 10^{-39}$, D = 10 km.

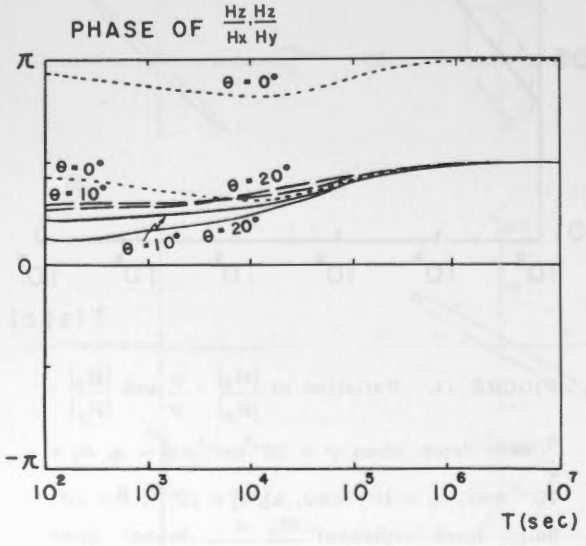

FIGURE 13. Phase difference of $\frac{H_z}{H_x}$, $\frac{H_z}{H_y}$ for $\nu = 10^{-7}\text{cm}^{-1}$, p = q, $\sigma_2 = 10^{-15}$emu, $\sigma_3 = 10^{-11}$ emu, $k_1^2/k_2^2 = 10^{-39}$, D = 10 km. Broken lines, $\frac{H_z}{H_x}$. Solid lines, $\frac{H_z}{H_y}$.

For the shorter periods $\frac{H_z}{H_y} \cdot \frac{q}{\nu}$ also increases as the depth to the conductor increases, as shown in Figure 14. The deeper the conductor, the less discernible any difference becomes between models of the tilted boundary and horizontal structure. When the depth is 10 km, the ratio for the tilted case for the period of 100 sec is 1.5 times as large as that of the horizontal case, whereas there is no significant difference between two models for the depth of 100 km.

c) Magnetotelluric relationship

The ratios of the electric field to the magnetic field variation, $\frac{E_x}{H_y}$ and $\frac{E_y}{H_x}$, are plotted against period for three

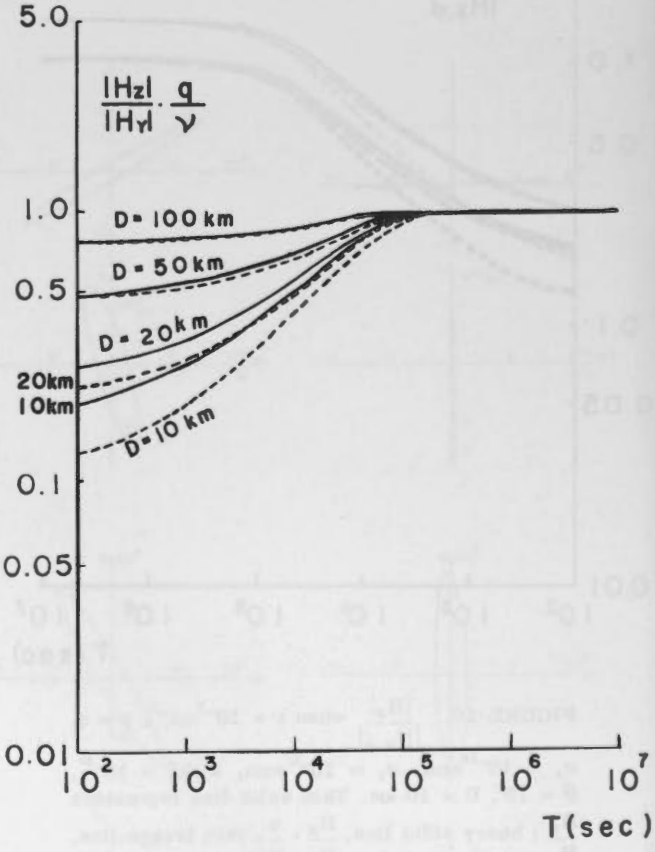

FIGURE 14. Variation of $\frac{|H_z|}{|H_y|} \cdot \frac{q}{\nu}$ with depth in the case where $\nu = 10^{-7}\text{cm}^{-1}$, p = q, $\sigma_2 = 10^{-15}$emu, $\sigma_3 = 10^{-11}$emu, $k_1^2/k_2^2 = 10^{-39}$ and $\theta = 0°$, 10°. Broken lines are for $\theta = 0°$, solid lines for $\theta = 10°$.

angles of tilt in Figures 15 and 16 for the model B ($\nu = 10^{-7}$ cm^{-1}, p = q). For periods less than 10^5 seconds, it is seen that $\frac{E_y}{H_x}$ is markedly influenced (a factor of two at T = 1000 sec) by an increase in tilt angle from $\theta = 0°$ to $\theta = 20°$, whereas E_x/H_y is relatively independent of tilt.

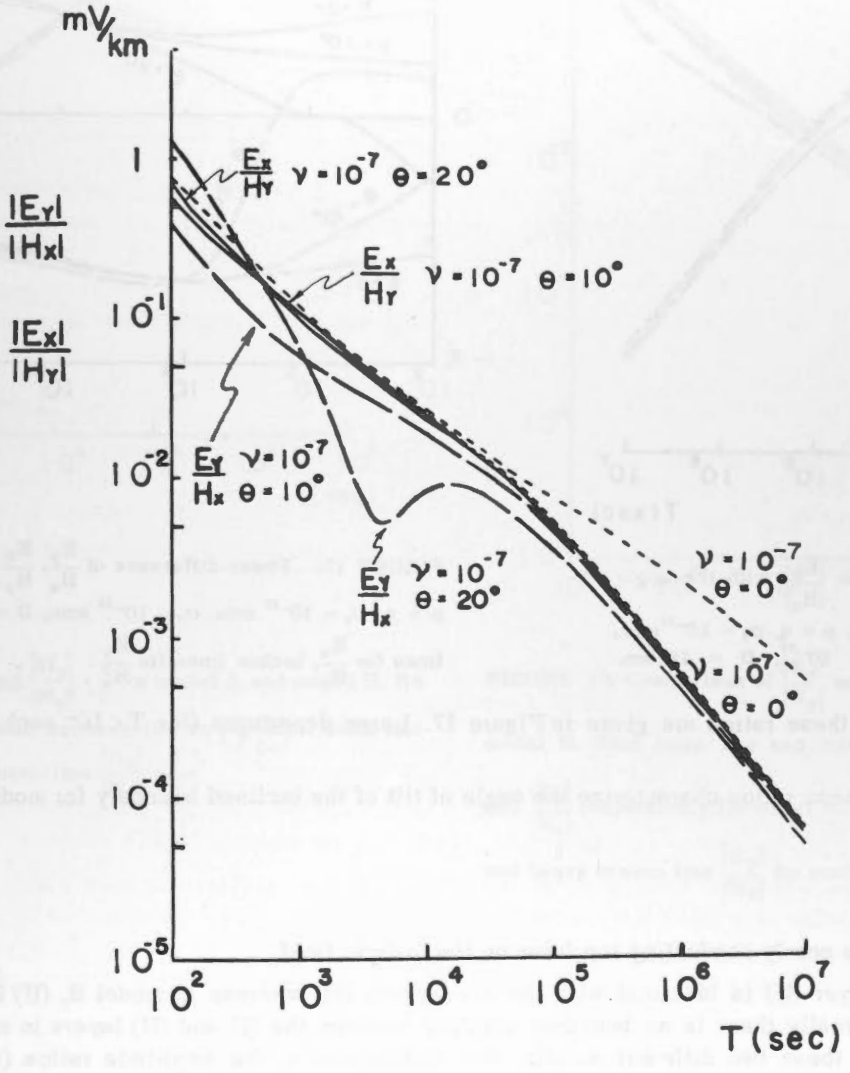

FIGURE 15. $\left|\frac{E_x}{H_y}\right|$ and $\left|\frac{E_y}{H_x}\right|$ for $\nu = 10^{-7}$ cm^{-1}, p = q, $\sigma_2 = 10^{-15}$ emu, $\sigma_3 = 10^{-11}$ emu, $k_1^2/k_2^2 = 10^{-39}$, $\theta = 10^0$, D = 10 km. Broken lines represent $\frac{E_y}{H_x}$, solid lines $\frac{E_x}{H_y}$. Dotted lines $\frac{E_x}{H_y}$, $\frac{E_y}{H_x}$ for $\theta = 0^0$.

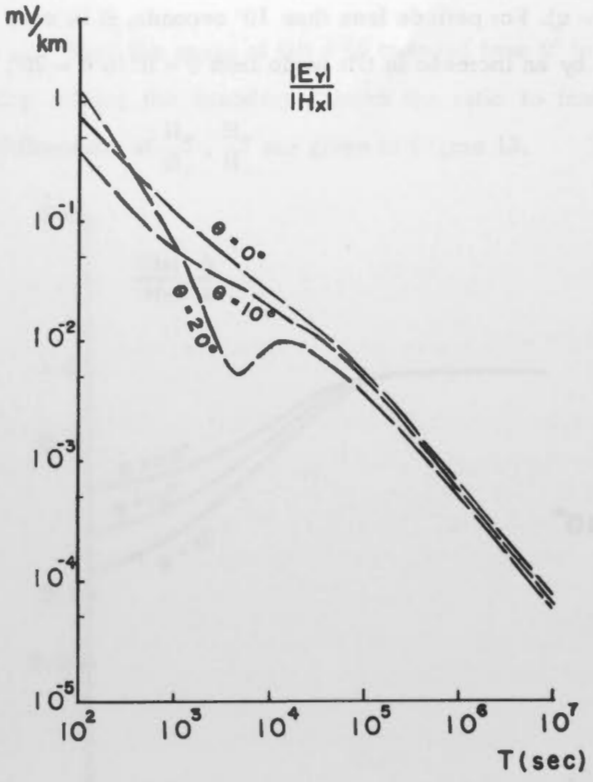

FIGURE 16. Variation in $\frac{|E_y|}{|H_x|}$ with the angle of tilt when $\nu = 10^{-7}\text{cm}^{-1}$, p = q, $\sigma_2 = 10^{-15}$emu, $\sigma_3 = 10^{-11}$emu, $k_1^2/k_2^2 = 10^{-39}$, D = 10 km.

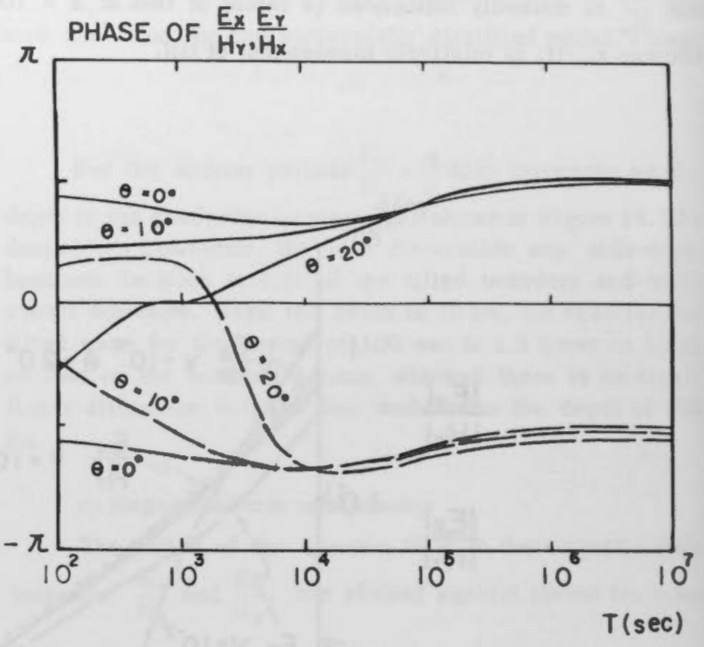

FIGURE 17. Phase difference of $\frac{E_y}{H_x}, \frac{E_x}{H_y}$ $\nu = 10^{-7}$ cm^{-1}, p = q, $\sigma_2 = 10^{-15}$ emu, $\sigma_3 = 10^{-11}$ emu, D = 10 km. Solid lines for $\frac{E_x}{H_y}$, broken lines for $\frac{E_y}{H_x}$.

Phase differences of these ratios are given in Figure 17. Large departures (for $T < 10^4$ sec) from the horizontal case are indicated.

One can deduce that these ratios characterize the angle of tilt of the inclined boundary for model B.

d) The influence of the poorly conducting top layer on the telluric field

In model A the top layer (II) is identical with the atmosphere (I), whereas in model B, (II) is a poor conductor in which $\sigma_2 = 10^{-15}$ emu. Actually there is no boundary existing between the (I) and (II) layers in model A. Numerical calculations were made for these two different models. Any differences in the amplitude ratios (see Figure 18) and phase differences of H_z/H_x and H_z/H_y were less than 10^{-3}. However, the magnetotelluric relationships, E_x/H_y and E_y/H_x, become different for short period variations as shown in Figure 19 and Figure 20. Anisotropic variation is rather conspicuous for the model B in this case. Consequently it may be concluded that the telluric variation is more sensitive to the change in conductivities between the model A and model B, although these two models are nearly identical so far as the magnetic variation is concerned. This result would be expected physically.

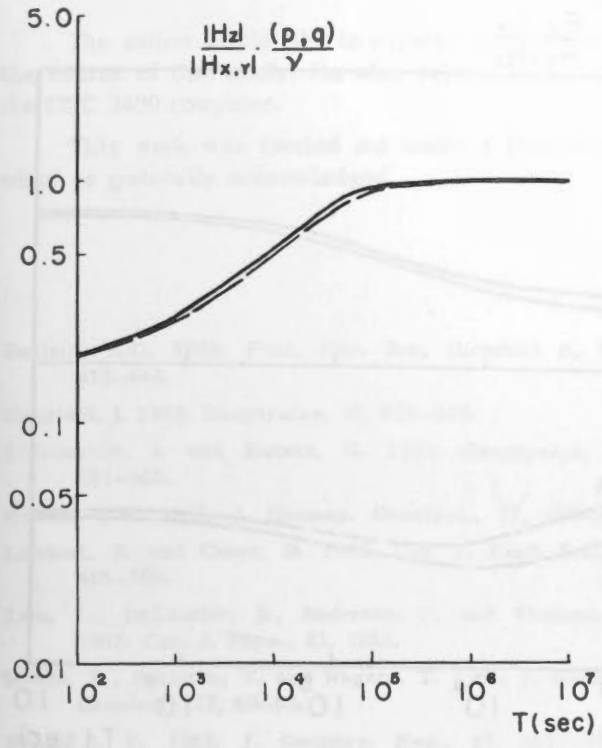

FIGURE 18. $\frac{|H_z|}{|H_x|}\cdot\frac{p}{\nu}$ and $\frac{|H_z|}{|H_y|}\cdot\frac{q}{\nu}$ for model A and model B. No difference is recognizable between the two models. Solid line represents $\frac{|H_z|}{|H_y|}\cdot\frac{q}{\nu}$, broken line $\frac{|H_z|}{|H_x|}\cdot\frac{p}{\nu}$.

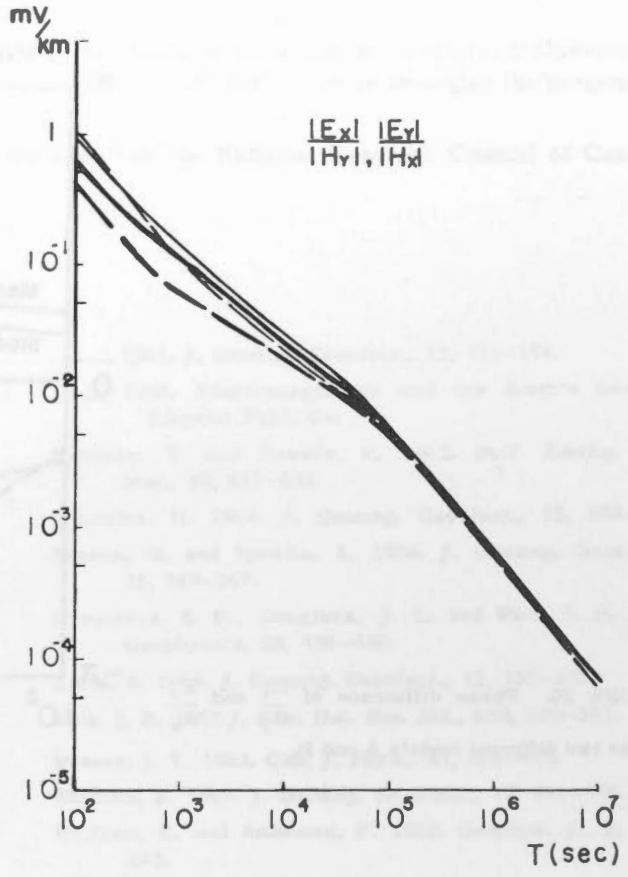

FIGURE 19. Comparison of $\frac{|E_x|}{|H_y|}$ and $\frac{|E_y|}{|H_x|}$ between model A and model B. Thin solid line and thin broken line represent $\frac{|E_x|}{|H_y|}$ and $\frac{|E_y|}{|H_x|}$ respectively for model A. Heavy solid line shows $\frac{|E_x|}{|H_y|}$ and heavy broken line $\frac{|E_y|}{|H_x|}$ for model B.

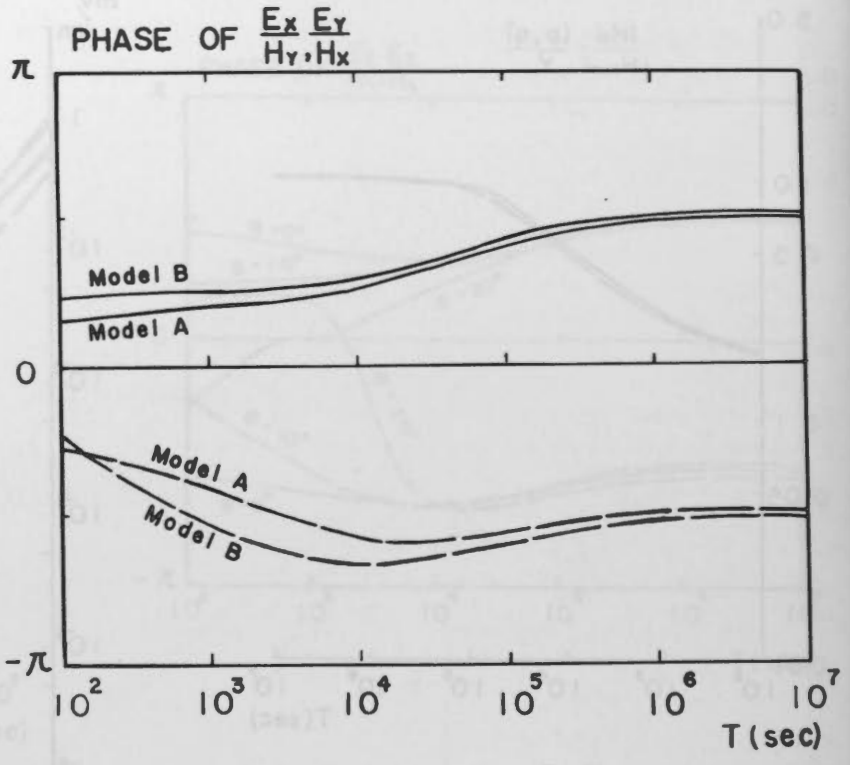

FIGURE 20. Phase difference of $\frac{E_x}{H_y}$ and $\frac{E_y}{H_x}$ for the two different models A and B.

6. Conclusions

The tilted boundary problem is essentially different from that of the horizontally stratified structure in the generation and coupling of the first and the second type field within the region bounded by the horizontal ground surface and the inclined boundary. The effect of the second type field is more serious on the electric field than on the magnetic field. It contributes to produce an anisotropic variation in the electric field.

A tilt of a highly conducting layer underlying an insulator or a poor conductor (model A and B) tends to confine the magnetic variation to a plane parallel to the inclined boundary itself. This has the effect of increasing the vertical component compared with the case of the horizontal conductor situated at the same depth. Such an increase becomes unrecognizable when the conductor is buried as deeply as 100 km under the ground for the model B ($\theta = 10^{\circ}$).

In a special case (model A) when the second layer (II) is identical with the atmosphere (I), (or a tilted conductor is exposed to the air), a strong confinement of the electric field in the y–direction was obtained. At the same time it has been shown that the magnetic variation is confined to a plane parallel to the tilted boundary. However the relationship between the limited direction of the electric field and the magnetic variation plane does not accord with the results of observations (Yokoyama 1961, 1962; Whitham and Andersen 1965).

When the second layer was replaced by a poorly conducting material (eg $\sigma_2 = 10^{-15}$ emu), the strong polarization of the electric field vanished, although there was still a noticeable anisotropic variation. This suggests that, however small the conductivity may be, the existence of a poor conductor different from the atmosphere, has some influence on the electromagnetic variation, and especially on the electric variation at the ground surface. This may be due to the large contrast of the parameter k between the atmosphere and the poor conductor (i. e. between k_1 and k_2) which tends to confine the second type field energy within the poorly conducting region (II).

The present theory, so long as the discussion is limited to a small angle of tilt ($\tan\theta < \frac{q}{\sqrt{\nu^2 + k_2^2}}$), does not sucessfully explain the observed strong polarization of the telluric field in connection with certain anomalous magnetic field variations, (eg Alert, N.W.T.) although some degree of anisotropy in the electric and the magnetic field has been theoretically obtained.

Acknowledgments

The author would like to express his sincere gratitude to Dr. K. Whitham for a number of helpful discussions in the course of this study. He also acknowledges the assistance of Mr. Jon M. DeLaurier in arranging the program for the CDC 3400 computer.

This work was carried out under a Postdoctorate Fellowship from the National Research Council of Canada, which is gratefully acknowledged.

References

Bullard, E.C. 1949. *Proc. Roy. Soc.* (London) A, **199**, 413–443.

Cagniard, I. 1953. *Geophysics*, **18**, 605–635.

D'Erceville, I. and Kunetz, G. 1962. *Geophysics*, **27**, 651–665.

Horton, C.W. 1965. *J. Geomag. Geoelect.*, **17**, 499–505.

Lambert, A. and Caner, B. 1965. *Can. J. Earth Sci.*, **2**, 485–509.

Law, L., DeLaurier, J., Andersen, F. and Whitham, K. 1963. *Can. J. Phys.*, **41**, 1868.

Maeda, R., Rikitake, T. and Nagata, T. 1965. *J. Geomag. Geoelect.*, **17**, 69–93.

Mann, J. E. 1964. *J. Geophys. Res.*, **69**, 3517–3524.

Niblett, E. R. and Sayn-Wittgenstein, C. 1960. *Geophysics*, **25**, 998–1008.

Parkinson, W.D. 1959. *Geophys. J.*, **2**, 1–14.

——— 1962. *Geophys. J.*, **4**, 441–449.

——— 1964. *J. Geomag. Geoelect.*, **65**, 222–226.

Price, A. T. 1950. *Quart. J. Mech. Appl. Math.*, **3**, 385–410.

1962. *J. Geophys. Res.*, **67**, 1907–1918.

Rankin, D. 1962. *Geophysics*, **27**, 666–676.

Rikitake, T. 1959. *Geophys. J.*, 276–287.

——— 1964. *J. Geomag. Geoelect.*, **15**, 181–184.

——— 1966. Electromagnetism and the Earth's Interior, Elsevier Publ. Co.

Rikitake, T. and Sawada, M. 1962. *Bull. Earthq. Res. Inst.*, **40**, 657–683.

Schmuker, U. 1964. *J. Geomag. Geoelect.*, **15**, 193–221.

Simeon, G. and Sposito, A. 1964. *J. Geomag. Geoelect.*, **15**, 249–267.

Srivastava, S. P., Douglass, J. L. and Ward, S. H. 1963. *Geophysics*, **28**, 426–446.

Kertz, W. 1964. *J. Geomag. Geoelect.*, **15**, 185–192.

Wait, J. R. 1962 *J. Res. Nat. Bur. Std.*, **660**, 509–541.

Weaver, J. T. 1963. *Can. J. Phys.*, **41**, 484–495.

Whitham, K. 1965. *J. Geomag. Geoelect.*, **17**, 481–498.

Whitham, K. and Andersen, F. 1962. *Geophys. J.*, **7**, 220–243.

——— 1965. *Geophys. J.*, **10**, 317–345.

Yokoyama, I. 1961. *J. Fac. Sci. Hokkaido Univ.*, Ser. VII. **1**, 331–346.

——— 1962. *J. Fac. Sci. Hokkaido Univ.*, Ser. VII. **1**, 393–403.

Yoshinatsu, T. 1957. *Mem. Kakioka Mag. Obs. Suppl.*, vol. 1. 1–76.